Gaussian theory for estimating fluctuating perturbations with backaction-evading oscillator variables

Jesper Hasseriis Mohr Jensen [*]
Department of Physics and Astronomy, Aarhus University, Ny Munkegade 120, DK-8000 Aarhus C, Denmark

Klaus Mølmer [†]
Aarhus Institute of Advanced Studies, Aarhus University, Høegh-Guldbergs Gade 6B, DK-8000 Aarhus C, Denmark and Center for Complex Quantum Systems, Department of Physics and Astronomy, Aarhus University, Ny Munkegade 120, DK-8000 Aarhus C, Denmark

(Received 27 March 2022; accepted 6 July 2022; published 25 August 2022)

We apply a Gaussian state formalism to track fluctuating perturbations that act on the position and momentum quadrature variables of a harmonic oscillator. Following a seminal proposal by Tsang and Caves [Phys. Rev. Lett. **105**, 123601 (2010)], Einstein-Podolsky-Rosen correlations with the quadrature variables of an ancillary harmonic oscillator are leveraged to significantly improve the estimates as relevant sensor variables can be arbitrarily squeezed while evading adverse effects from the conjugate, antisqueezed variables. Our real-time analysis of the continuous monitoring of the system employs a hybrid quantum-classical description of the quantum probe and the unknown classical perturbations, and it provides a general formalism to establish the achievements of the sensing scheme and how they depend on different parameters.

DOI: 10.1103/PhysRevA.106.022613

I. INTRODUCTION

The probabilistic nature of measurements on a quantum system and the disturbance of the system by measurement backaction puts intriguing limits on the sensitivity of measurement schemes. For measurements aiming to resolve candidate values of a classical perturbation that influences a quantum system, measurements of the same observable at different times thus face a conundrum: overly precise measurements at early times cause radical changes in the state of the quantum system and may hence hinder or seriously disrupt later precision measurements. Pioneering works by Braginsky, Thorne, Caves, and others [1–4] identified so-called quantum nondemolition (QND) measurement schemes, where the same observable can be repeatedly or continuously measured over time in a manner that accumulates sensitivity and gradually projects the system on an eigenstate. For canonical position and momentum variables, this is intimately connected with the concept of squeezing, which may be both a property of the initially prepared quantum probe system and an emergent property due to the measurement process itself. Notably, in the advanced Laser Interferometer Gravitational-Wave Observatory (LIGO) for gravitational wave detection one may use squeezed input states of light to enhance the interferometric sensing of the motion of test mass mirrors [5]. The test mass position and momentum variables, however, must obey the Heisenberg uncertainty relation, and strong position squeezing implies strong antisqueezing of the momentum observable and, hence, antisqueezing of later values of the position.

Replacing continuous probing by brief measurements every half-oscillation period presents a way to persistently squeeze a definite, rotating quadrature component of the oscillator [6]. Another elegant proposal employs an ancillary oscillator to form commuting pairs of observables $\hat{x}_- = (\hat{x}_1 - \hat{x}_2)/\sqrt{2}$ and $\hat{p}_+ = (\hat{p}_1 + \hat{p}_2)/\sqrt{2}$ which may be measured with arbitrary precision and which are not coupled to their conjugate observables if the two oscillators have opposite oscillator frequencies [7,8]. The ancillary system is then referred to as a negative-mass oscillator (its position changes according to the value of the negative of the momentum), and the observables $\hat{x}_-$, $\hat{p}_+$ are referred to as quantum-free or backaction-free. Following Refs. [7,8], and in independent work, use of this concept has been suggested for various scenarios [9–12]. The commuting collective observables at the heart of the backaction evasion mechanism are exactly those proposed in the famous foundational EPR paradox by Einstein, Podolsky, and Rosen [13], and previous proposals [14] and experiments [15] employing these states are, indeed, closely related to the proposal in Refs. [7,8]. For a pedagogical introduction and recent experiments, see Refs. [16,17].

The use of the backaction evasion mechanism is illustrated in Fig. 1. We imagine that the oscillator on the left is subject to perturbations that affect its position and momentum observables. By monitoring the collective EPR observables including the position and momentum of the ancillary oscillator, which is not affected by the perturbation, we squeeze both of these observables and we may infer the value of the perturbations with high precision. We sketch the probing by two light beams that undergo sequential coherent displacements proportional to the oscillator observables, and which are subsequently detected in a homodyne manner. As laid out

[*]jhasseriis@phys.au.dk
[†]moelmer@phys.au.dk

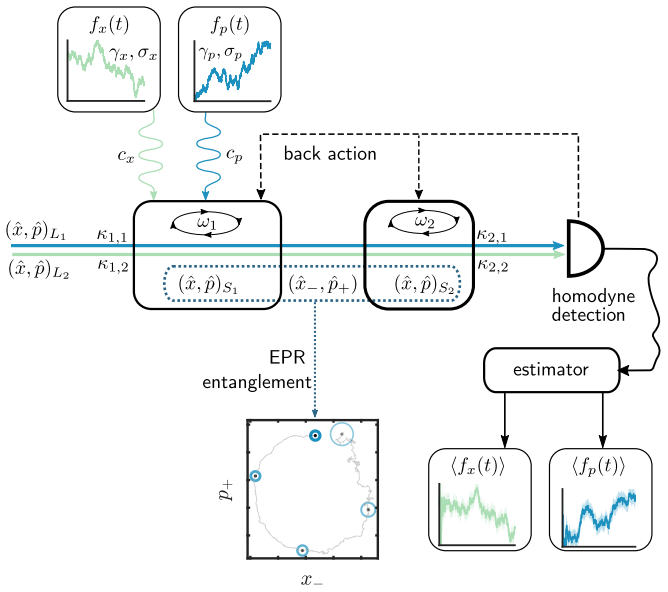

FIG. 1. Real-time tracking of two classical perturbations $f_x(t)$ and $f_p(t)$ acting on a single oscillator S_1. Collective EPR variables $\hat{x}_- \propto (\hat{x}_1 - \hat{x}_2)$ and $\hat{p}_+ \propto (\hat{p}_1 + \hat{p}_2)$ of S_1 and an ancillary oscillator S_2 are probed with two cw light beams L_1 and L_2. These variables commute and can be squeezed with no limits. Crucially, choosing opposite oscillator frequencies $\omega_1 = -\omega_2$ decouples $\hat{x}_-$ and $\hat{p}_+$ from the antisqueezed EPR variables $\hat{p}_-$ and $\hat{x}_+$. The time-evolved state has the initial oscillator ground-state correlations, $\Delta\hat{x}_1^2 = \Delta\hat{p}_1^2 = \Delta\hat{x}_2^2 = \Delta\hat{p}_2^2 = 1/2$ and the gradual squeezing of the EPR observables due to the measurements benefit the estimation of the perturbations $f_x(t)$ and $f_p(t)$. The noisy data displayed in the panels come from an actual numerical simulation.

in more detail in the following sections, the setup is described by the Hamiltonian

$$\begin{aligned}\frac{\hat{H}}{\hbar} &= \frac{1}{\hbar}\left(\hat{H}_{\omega_1,\omega_2} + \hat{H}_{\boldsymbol{\kappa}} + \hat{H}_{c_x,c_p}\right)\\ &\equiv \frac{\omega_1}{2}\left(\hat{x}_{S_1}^2 + \hat{p}_{S_1}^2\right) + \frac{\omega_2}{2}\left(\hat{x}_{S_2}^2 + \hat{p}_{S_2}^2\right)\\ &\quad + \left(\kappa_{1,1}\hat{p}_{S_1} + \kappa_{2,1}\hat{p}_{S_2}\right)\hat{p}_{L_1}\\ &\quad + \left(\kappa_{1,2}\hat{x}_{S_1} + \kappa_{2,2}\hat{x}_{S_2}\right)\hat{x}_{L_2}\\ &\quad - c_x f_x \hat{x}_{S_1} + c_p f_p \hat{p}_{S_1}, \end{aligned} \tag{1}$$

where ω_i are oscillator frequencies, $\kappa_{i,j}$ are light coupling strengths, and c_q are perturbation coupling strengths (for $i, j = 1, 2$ and $q = x, p$). The setup is generic for a range of physical systems including mechanical and collective spin oscillators, probed by optical phase shifts or Faraday rotation angles, but we assume Gaussian states (Sec. II), including coherent, squeezed, and thermal states [18], and we also assume that the perturbing forces or fields are governed by Gaussian statistics (Sec. III).

The purpose of this article is twofold. On the one hand we present an analysis and we provide tools to model the specific backaction-evading probe scheme depicted in Fig. 1 (Sec. IV). On the other hand we introduce and demonstrate the application of the Gaussian state formalism in full generality to describe both unitary interactions and homodyne detection and to model the estimation of constant or fluctuating classical perturbations. We "quantize" the values of the classical perturbations, i.e., we associate them with QND degrees of freedom of fictitious ancillary quantum systems.

Both for the specific scheme of interest and for a variety of other sensing models, our hybrid quantum-classical description makes the Bayesian update of the classical likelihood distribution equivalent to the quantum backaction on the combined quantum state. This approach thus permits inclusion of Gaussian classical parameters in the Gaussian quantum state formalism on equal footing with the sensor quantum observables. In particular, we characterize the entire set of quantum and classical variables by mean values and a covariance matrix, which explicitly includes estimators of the perturbations and their corresponding Gaussian variances.

To make our presentation self-contained, we present, derive, and explain several elements of the physical modeling of the continuous interrogation of the oscillator systems. In this way we show how the formalism readily permits the gradual inclusion of the more specific elements of the scheme illustrated in Fig. 1, and how it may be readily applied to a variety of other oscillator systems and observables. In a series of articles [19–21], Tsang derived equivalent equations, and we refer, in particular, to Table 1 of Ref. [20] for a summary of the connections between the theory of classical estimation theory by Kalman filters [22] and smoothers [23,24] and the formal elements of the quantum theory with Gaussian states and operations. See also Ref. [25] which elaborates on the connection to measurement effect operators for continuous probing as promoted in Ref. [26].

The article is structured as follows: In Sec. II we introduce the Gaussian state formalism and derive equations of evolution for the first and second moments of Gaussian distributions due to interactions and continuous probe measurements. In Sec. III we represent classical perturbations as eigenvalues of observables for which the system is in a purely diagonal, mixed state, and we derive a quantum-classical hybrid formalism for the joint, conditional probability of all variables. The methods and results of Secs. II and III are general and apply to a host of systems and measurement scenarios. This includes the extension to smoothed estimates which generalize classical smoothing filters to application with quantum probes. In Sec. IV we discuss a number of numerical examples of our formalism, and we arrive at quantitative evidence for the advantages of backaction-evading probing schemes. Section V concludes the article and provides a summary and an outlook with emphasis on the challenges posed by systems that are not described by Gaussian variables.

II. GAUSSIAN STATE FORMALISM

Parameter estimation by continuous probing of a quantum probe system is described by the Belavkin filter [27]. This theory applies quantum trajectory theory and generic conditional density matrices [19,28,29], while the restriction to Gaussian states and operations implies a significant reduction in numerical complexity. The Gaussian description applies to the harmonic-oscillator variables of the scheme presented in Fig. 1.

A. Gaussian states

Consider a collection of n canonical degrees of freedom represented by the vector of operators,

$$\hat{\boldsymbol{y}} = (\hat{x}_1, \hat{p}_1, \ldots, \hat{x}_n, \hat{p}_n)^T, \tag{2}$$

where $[\hat{x}_i, \hat{p}_j] = i\hbar\delta_{ij}$. Any operator $\hat{A}$ defined on this continuous variable system space, and in particular the density operator $\hat{A} = \hat{\rho}$ describing the quantum state, can be represented, e.g., in the position eigenbasis $\langle \boldsymbol{x}|\hat{\rho}|\boldsymbol{x}'\rangle$, and it has an equivalent representation in terms of its Wigner function,

$$\mathcal{W}_{\hat{\rho}}(\boldsymbol{y}) = \frac{1}{(\hbar\pi)^n}\int \langle \boldsymbol{x}+\boldsymbol{q}\,|\,\hat{\rho}\,|\,\boldsymbol{x}-\boldsymbol{q}\rangle e^{2i\boldsymbol{p}\cdot\boldsymbol{q}/\hbar}\,d\boldsymbol{q}, \tag{3}$$

where $\boldsymbol{x} = (x_1, \ldots, x_n)^T$ and $\boldsymbol{p} = (p_1, \ldots, p_n)^T$, and $d\boldsymbol{q} = dq_1 \cdots dq_n$ denotes integration over all position variable arguments $\boldsymbol{q}$. The Wigner function is a normalized quasiprobability distribution, whose value at a single point entails definite values of noncommuting variables and is hence not directly meaningful. Still the Wigner function permits calculation of expectation values as weighted "phase space" integrals,

$$\langle \hat{A}\rangle_{\hat{\rho}} = \mathrm{tr}[\hat{A}\hat{\rho}] = (\hbar\pi)^n \int \mathcal{W}_{\hat{A}}\mathcal{W}_{\hat{\rho}}\,d\boldsymbol{y}, \tag{4}$$

and the special case of a projection on a definite quadrature eigenstate $\hat{A} = |y_j\rangle\langle y_j|$ yields the marginal density for measurements of y_j by integrating all coordinates except y_j,

$$P(y_j) = \mathrm{tr}[|y_j\rangle\langle y_j|\hat{\rho}] = \int \mathcal{W}_{\hat{\rho}}\,d\boldsymbol{y}_{i\neq j}. \tag{5}$$

The Wigner function for the reduced density matrix after the partial trace over the nth mode, $\mathrm{tr}_n\rho$, is similarly given by an integral, e.g., for two modes,

$$\mathcal{W}_{\mathrm{tr}_2\hat{\rho}}(x_1, p_1) = \int \mathcal{W}_{\hat{\rho}}(x_1, p_1, x_2, p_2)\,dx_2 dp_2. \tag{6}$$

The Wigner function of an arbitrary quantum state is generally a complex object, but Gaussian states, i.e., states with Gaussian Wigner functions,

$$\mathcal{W}^{\boldsymbol{m},\boldsymbol{\Gamma}}_{\hat{\rho}}(\mathbf{y}) = \frac{1}{(\hbar\pi)^n}\frac{e^{-(\mathbf{y}-\boldsymbol{m})^T\boldsymbol{\Gamma}^{-1}(\mathbf{y}-\boldsymbol{m})}}{\sqrt{\det\boldsymbol{\Gamma}}}, \tag{7}$$

are fully characterized by their first and second moments, i.e., by a vector of mean values and a covariance matrix,

$$\boldsymbol{m} = \langle\hat{\mathbf{y}}\rangle, \tag{8}$$

$$\Gamma_{i,j} = 2\mathrm{Re}(\langle\hat{y}_i\hat{y}_j\rangle - \langle\hat{y}_i\rangle\langle\hat{y}_j\rangle), \quad i,j = 1,\ldots,2n. \tag{9}$$

The variance of a quantum variable is $\Delta\hat{y}_j^2 \equiv \Delta(\hat{y}_j, \hat{y}_j) = \frac{1}{2}\Gamma_{j,j}$, and we shall refer to covariance matrix elements either by their vector indices or variable names, for example $m_2 = m_{p_1}$ and $\Gamma_{1,4} = \Gamma_{x_1,p_2}$.

The partial trace over some modes is effectively achieved by simply removing their corresponding entries in the covariance matrix $\boldsymbol{\Gamma}$ and mean vector $\boldsymbol{m}$, and, e.g., the marginal density of any single quadrature observable is a univariate Gaussian,

$$P(y_j) = \int \mathcal{W}^{\boldsymbol{m},\boldsymbol{\Gamma}}_{\hat{\rho}}(\mathbf{y})\,d\mathbf{y}_{i\neq j} = \mathcal{N}\left(m_j, \frac{\Gamma_{j,j}}{2}\right), \tag{10}$$

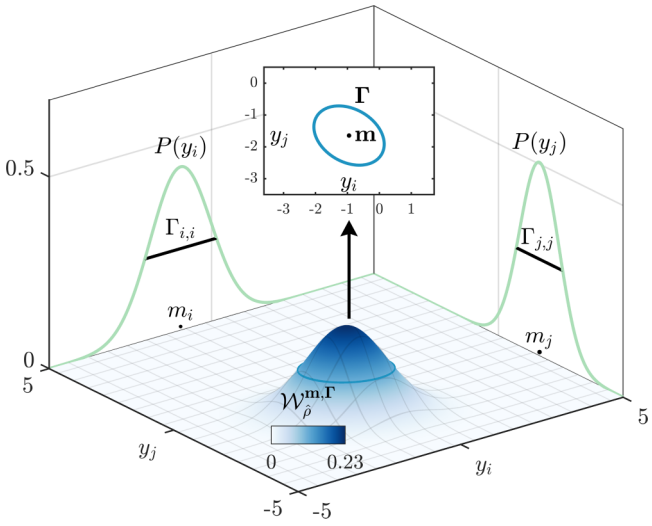

FIG. 2. Illustration of a Gaussian state with a joint marginal probability density of two observables y_i, y_j. The density is parametrized by $\boldsymbol{m} = \left(\begin{smallmatrix}-0.95\\-1.65\end{smallmatrix}\right)$ and $\boldsymbol{\Gamma} = \left(\begin{smallmatrix}1.75 & -0.43\\-0.43 & 1.24\end{smallmatrix}\right)$, and the contour line at half maximum (ellipses) and mean (dots) are depicted in two dimensions in the inset. The marginal densities of y_k are centered on $\boldsymbol{m}_k$ with variances $\Gamma_{k,k}$ (for $k = i, j$).

where $\mathcal{N} \propto \exp[-(y_j - m_j)^2/\Gamma_{j,j}]$. An illustration of how marginal densities are related to joint densities is depicted for two variables in Fig. 2.

Operations that preserve the Gaussian form of the Wigner function are fully represented by their transformation of the first and second moments. Knowledge of these transformations are sufficient to describe the detection scheme in Fig. 1 as detailed below.

B. Time evolution

Heisenberg's equation of motion applies for all quadrature observables and for a small time step δt,

$$\hat{y}_j(t+\delta t) \approx \hat{y}_j(t) + \dot{\hat{y}}_j(t)\delta t = \hat{y}_j(t) + \frac{i}{\hbar}[\hat{H}(t), \hat{y}_j(t)]\delta t. \tag{11}$$

If the Hamiltonian $\hat{H}$ is at most quadratic in the quadrature operators $\hat{\mathbf{y}}$, as is the case in (1), the unitary time evolution results in an affine transformation of the observables in the Heisenberg picture,

$$\hat{\mathbf{y}}(t+\delta t) = \boldsymbol{S}_{\delta t}\hat{\mathbf{y}}(t) + \boldsymbol{F}_{\delta t}, \tag{12}$$

and to first order in δt the corresponding evolution of the first and second moments yields

$$\boldsymbol{m}(t+\delta t) = \boldsymbol{S}_{\delta t}\boldsymbol{m}(t) + \boldsymbol{F}_{\delta t}, \tag{13a}$$

$$\boldsymbol{\Gamma}(t+\delta t) = \boldsymbol{S}_{\delta t}\boldsymbol{\Gamma}(t)\boldsymbol{S}_{\delta t}^T. \tag{13b}$$

We note that $\boldsymbol{S}_{\delta t}$ and $\boldsymbol{F}_{\delta t}$ may be time-dependent matrices if the Hamiltonian contains time-dependent driving or coupling terms. In addition to the Hamiltonian interaction, the system may be subject to dissipation and fluctuations, imposing damping rates for the mean values and covariance matrix elements and diffusive spreading for the variances. For

our application, these effects can be described by a diagonal damping matrix $\boldsymbol{D}_{\delta t}$ and a diagonal diffusion matrix $\boldsymbol{L}_{\delta t}$, such that $\boldsymbol{S}_{\delta t} \to \boldsymbol{D}_{\delta t}\boldsymbol{S}_{\delta t}$ in Eqs. (13a) and (13b), and $\boldsymbol{L}_{\delta t}$, is added on the right-hand side in the update of $\boldsymbol{\Gamma}$ in (13b). We refer to Sec. IV A for the specific expression for $\boldsymbol{D}_{\delta t}$ and $\boldsymbol{L}_{\delta t}$ pertaining to the setup in Fig. 1.

C. Measurement of some quadratures observables

Suppose the system is divided into subsystems A and B with n_A and n_B oscillator modes, such that we may write

$$\hat{\boldsymbol{y}} = \begin{pmatrix} \hat{\boldsymbol{y}}_A \\ \hat{\boldsymbol{y}}_B \end{pmatrix},$$

where $\hat{\boldsymbol{y}}_A = (\hat{x}_1, \hat{p}_1, \ldots, \hat{x}_{n_A}, \hat{p}_{n_A})^T$ is of length $2n_A$ and $\hat{\boldsymbol{y}}_B = (\hat{x}_{n_A+1}, \hat{p}_{n_A+1}, \ldots, \hat{x}_n, \hat{p}_n)^T$ is of length $2n_B$. The Gaussian moments may then be similarly divided,

$$\boldsymbol{m} = \begin{pmatrix} \boldsymbol{a} \\ \boldsymbol{b} \end{pmatrix}, \quad \boldsymbol{\Gamma} = \begin{pmatrix} \boldsymbol{A} & \boldsymbol{C} \\ \boldsymbol{C}^T & \boldsymbol{B} \end{pmatrix}. \tag{14}$$

$\boldsymbol{A}$ is the $2n_A \times 2n_A$ covariance matrix for the variables $\hat{\boldsymbol{y}}_A$, $\boldsymbol{B}$ is the $2n_B \times 2n_B$ covariance matrix for the variables $\hat{\boldsymbol{y}}_B$, while $\boldsymbol{C}$ is the $2n_A \times 2n_B$ covariance matrix describing the correlations, or entanglement, between the two subsystems A and B.

We already discussed how the reduced density matrix and Wigner function of one subsystem is obtained by retaining only the relevant mean values and covariance elements, say, $\boldsymbol{a}$ and $\boldsymbol{A}$, when B is traced out. Consider now instead the state of the same subsystem, but conditioned on a projective quadrature measurement of all n_B oscillator modes in subsystem B. If the two sets of subsystems are correlated, i.e., $\boldsymbol{C}$ is nonzero, the outcome of this measurement will influence the resulting state of subsystem A through measurement backaction. This can be understood from the inset in Fig. 2 where a measurement of the variable y_j causes the y_i distribution to have equal values at the intersection of the contour ellipse and a horizontal line at the random outcome $y_j = y_j^{\text{meas}}$.

Assuming classical (commuting) variables, for the measurement of $\boldsymbol{y}_B$, the restriction of the corresponding arguments in (7) to their measured values is a Gaussian function of the remaining variables $\boldsymbol{y}_A$ with the coefficients of the appropriate block submatrix of $\boldsymbol{\Gamma}^{-1}$. The corresponding reduced covariance matrix, in turn, is the inverse of that submatrix. By linear algebra, the inversion of the block matrix $\boldsymbol{\Gamma}$ (14), thus yields the conditional covariance matrix, $\boldsymbol{A}^{\text{cond}} = \boldsymbol{A} - \boldsymbol{C}\boldsymbol{B}^{-1}\boldsymbol{C}^T$ and vector of mean value, $\boldsymbol{a}^{\text{cond}} = \boldsymbol{a} + \boldsymbol{C}\boldsymbol{B}^{-1}(\boldsymbol{y}^{\text{meas}} - \boldsymbol{b})$ [30].

In the quantum setting, we cannot simultaneously measure both but only one of the x or p quadratures of the $\hat{\boldsymbol{y}}_B$ variables while the canonically conjugate, unmeasured quadrature variables become completely uncertain due to the Heisenberg uncertainty relation. In this case we have recourse to an appropriately modified transformation of the conditional moments for subsystem A,

$$\boldsymbol{A}^{\text{cond}} = \boldsymbol{A} - \boldsymbol{C}(\boldsymbol{\Pi}\boldsymbol{B}\boldsymbol{\Pi})^{-}\boldsymbol{C}^T, \tag{15a}$$

$$\boldsymbol{a}^{\text{cond}} = \boldsymbol{a} + \boldsymbol{C}(\boldsymbol{\Pi}\boldsymbol{B}\boldsymbol{\Pi})^{-}\boldsymbol{\Delta}_B^{\text{meas}}, \tag{15b}$$

where $(\cdot)^{-}$ denotes the Moore-Penrose pseudoinverse of its matrix argument (see Ref. [31] for a general discussion of the backaction of quadrature measurements on Gaussian states). The projection matrix $\boldsymbol{\Pi}$ is a block matrix formed by subprojectors

$$\boldsymbol{\pi}_i \in \{\boldsymbol{\pi}_x, \boldsymbol{\pi}_p\} \equiv \left\{ \begin{pmatrix} 1 & 0 \\ 0 & 0 \end{pmatrix}, \begin{pmatrix} 0 & 0 \\ 0 & 1 \end{pmatrix} \right\}, \tag{15c}$$

assuming the measured quadrature for each mode $i = 1, \ldots, n_B$ in $\hat{\boldsymbol{y}}_B$ is either the position or momentum. The measurement outcomes $q_i^{\text{meas}} = (q_1, \ldots, q_{n_B})$ form a vector that can be written as the diagonal elements of a block matrix $\text{diag}(\oplus_i q_i^{\text{meas}}\boldsymbol{\pi}_i)$, where $q \in \{x, p\}$ is the quadrature designated by $\boldsymbol{\pi}_i$. Defining a similar vector of the expectation values $\langle \hat{q}_i \rangle$ of the same quantities (given by the corresponding entries of $\boldsymbol{b}$), we define their difference

$$\boldsymbol{\Delta}_B^{\text{meas}} = \text{diag}\big[\oplus_i \big(q_i^{\text{meas}} - \langle \hat{q}_i \rangle\big)\boldsymbol{\pi}_i \big]. \tag{15d}$$

See Sec. IV A for the application to the setup in Fig. 1.

D. Continuous monitoring

We are interested in the case where the subsystem B, used to probe subsystem A, forms a continuous-wave (cw) light beam in a coherent state, consistent with a Gaussian state description. To encompass both the continuous unitary evolution and evolution due to the interaction and the measurement backaction we represent a continuous probe beam as a "train" of very short segments of duration δt, each treated as a single mode, and interacting sequentially with system A [32]. Similar steps are followed in the derivation presented in Ref. [26]. Each field segment is initially in the same (trivial) coherent field state and is not correlated with system A prior to their interaction. The assumption of coherent states implies that there are no correlations between the incident light segments.

Once a light segment arrives, it takes the role as subsystem B in Eqs. (14) with covariance matrices and mean values,

$$\boldsymbol{B} \to \mathbb{1}_{2n_B \times 2n_B}, \tag{16a}$$

$$\boldsymbol{C} \to \mathbb{O}_{2n_A \times 2n_B}, \tag{16b}$$

$$\boldsymbol{b} \to \mathbb{O}_{2n_B \times 1}, \tag{16c}$$

where $\mathbb{1}$ and $\mathbb{O}$ are the identity and zero matrices of the indicated dimensions. The system and the light segment interact briefly by Eqs. (13), and the latter is subsequently subject to a homodyne measurement with an associated backaction on system A given by Eqs. (15),[1] whence the projected field quadrature eigenstate factors and disappears from the description. The effective $t \to t + \delta t$ evolution of system A can hence be summarized as

$$\boldsymbol{a}(t) \overset{(13)}{\to} \boldsymbol{a}(t+\delta t) \overset{(15)}{\to} \boldsymbol{a}^{\text{cond}}(t+\delta t) \equiv \boldsymbol{a}(t+\delta t), \tag{16d}$$

$$\boldsymbol{A}(t) \to \boldsymbol{A}(t+\delta t) \to \boldsymbol{A}^{\text{cond}}(t+\delta t) \equiv \boldsymbol{A}(t+\delta t). \tag{16e}$$

This process is then repeated with the next "fresh" incident light segments, and application of Eqs. (16) yields the continued evolution of subsystem A due to the interactions and accumulation of probe measurement data.

[1]The pseudoinverse of B is approximated to lowest order by $(\boldsymbol{\Pi}\boldsymbol{B}\boldsymbol{\Pi})^{-} \approx \boldsymbol{\Pi}$ with corrections $O(\delta t)$ due to the interaction.

The continuous detection record that conditions the dynamics,

$$\boldsymbol{q}_B^{\text{meas}}(t) = \big(q_1, \ldots, q_{n_B}\big), \tag{17a}$$

may be extracted from an actual experiment or, in the event of a purely numerical simulation, be sampled from a normal distribution

$$q_i \sim \mathcal{N}\big(\langle \hat{q}_i \rangle,\ \Delta \hat{q}_i^2\big) \approx \mathcal{N}(\langle \hat{q}_i \rangle,\, 1/2). \tag{17b}$$

The expectation value $\langle \hat{q}_i \rangle$ and variance $\Delta \hat{q}_i^2$ are elements of $\boldsymbol{b}$ and $\boldsymbol{B}$ after the interaction, respectively, and the approximation $\Delta \hat{q}_i^2 = 1/2$ holds for the infinitesimal interaction with light segments of short duration.

We note that the covariance matrix update (15a) does not depend on the actual measurement outcome, and in the limit of infinitesimally small time steps, $\boldsymbol{A}$ it becomes the solution of a Riccati matrix differential equation [32],

$$\dot{\boldsymbol{A}} = \lim_{\delta t \to 0^+} \frac{\boldsymbol{A}(t+\delta t) - \boldsymbol{A}(t)}{\delta t} \tag{18}$$

$$\equiv \boldsymbol{G} - \boldsymbol{D}\boldsymbol{A} - \boldsymbol{A}\boldsymbol{E} - \boldsymbol{A}\boldsymbol{F}\boldsymbol{A}, \tag{19}$$

where the matrices $\boldsymbol{G}, \boldsymbol{D}, \boldsymbol{E}, \boldsymbol{F}$ are determined from the physical interactions leading to the dynamics. The nonlinear matrix Riccati equation can be decomposed into $\boldsymbol{A} = \boldsymbol{W}\boldsymbol{U}^{-1}$ where $\boldsymbol{W}$ and $\boldsymbol{U}$ are solutions to two linear matrix equations $\dot{\boldsymbol{W}} = -\boldsymbol{D}\boldsymbol{W} + \boldsymbol{G}\boldsymbol{U}$ and $\dot{\boldsymbol{U}} = \boldsymbol{F}\boldsymbol{W} + \boldsymbol{E}\boldsymbol{U}$. Expressions for the matrices $\boldsymbol{G}, \boldsymbol{D}, \boldsymbol{E}, \boldsymbol{F}$ for our specific system are presented in the Appendix.

III. ESTIMATION OF CLASSICAL PERTURBATIONS WITH CONTINUOUS MONITORING

A perturbation of the oscillator system, caused, e.g., by classical forces or external fields $f_i(t)$ will result in a proportional displacement of the oscillator quadratures. In this article, we assume that each of the, say, n_f perturbations are individually characterized by a time-dependent Ornstein-Uhlenbeck (OU) process,

$$df_i(t) = -\gamma_i f_i(t) dt + \sqrt{\sigma_i} dW_i(t), \quad i = 1, \ldots, n_f. \tag{20}$$

The OU process is damped with a rate γ_i and undergoes diffusion governed by a diffusion constant σ_i and stochastic Wiener increments, $dW_i(t) \sim \mathcal{N}(0, dt)$. We may readily include the effect on the quantum observables of such a *known* time-dependent perturbation through the appropriate entries in $\boldsymbol{F}_{\delta t}$ in Eq. (13a), and Sec. II D provides the quantum dynamics (16) conditioned on any specified perturbation and an observed detection record (17).

However, we wish to estimate an *unknown* time-dependent perturbation from the measurements. Hence rather than the f_i's being known we represent them by probability distributions and infer their evolution due to the acquisition of measurement data. This is done conveniently by incorporating the evolution of these distributions into the already established quantum formalism.

Equation (20) is equivalent to a Fokker-Planck equation describing the probability density of the value of $f_i(t)$, which takes a Gaussian form. We shall use this fact to enable a formal description of the unknown perturbations at the level of Gaussian Wigner functions and quantum density operators.

A. Filtering

1. Quantum-classical hybrid formalism

It is convenient to introduce for each perturbation f_i an ancillary quantum operator $\hat{f}_i$ and specify its eigenstates, $\hat{f}_i|f_i\rangle = f_i|f_i\rangle$, with eigenvalues for each possible value of f_i. In this way, a classical probability density $P(\boldsymbol{f} = (f_1, f_2, \ldots, f_{n_f}))$ can be represented as a quantum state in an incoherent mixture of eigenstates, $\hat{\chi} = \int d\boldsymbol{f} |\boldsymbol{f}\rangle\langle\boldsymbol{f}| P(\boldsymbol{f})$ with $|\boldsymbol{f}\rangle = \otimes_{i=1}^{n_f} |f_i\rangle$.

We may then define an augmented density operator [note the "$\sim$"] on the joint space of ancillary and genuine quantum variables,

$$\hat{\tilde{\rho}} = \int d\boldsymbol{f}\, |\boldsymbol{f}\rangle\langle\boldsymbol{f}| \otimes \hat{\rho}_{\boldsymbol{f}}, \tag{21}$$

where $\hat{\tilde{\rho}}(0) = \hat{\chi} \otimes \hat{\rho}(0)$ for some initial state $\hat{\rho}(0)$ on the space of genuine quantum variables.[2] In Eq. (21) the probability density $P(\boldsymbol{f})$ is absorbed in the norm of $\hat{\rho}_{\boldsymbol{f}}$ and can be retrieved by standard quantum expressions

$$P(\boldsymbol{f}) = \text{tr}[|\boldsymbol{f}\rangle\langle\boldsymbol{f}|\hat{\tilde{\rho}}] = \text{tr}[\hat{\rho}_{\boldsymbol{f}}], \tag{22}$$

$$P(f_j) = \text{tr}[|f_j\rangle\langle f_j|\hat{\tilde{\rho}}] = \int d\boldsymbol{f}_{i\neq j}\, \text{tr}[\hat{\rho}_{\boldsymbol{f}}], \tag{23}$$

where $\boldsymbol{f}_{i\neq j}$ denotes all components of $\boldsymbol{f}$ except f_j, and "tr" denotes the trace over all degrees of freedom of its operator argument, which differ in the second and last terms of Eqs. (22) and (23). The time evolution of each $\hat{\rho}_{\boldsymbol{f}}$ is conditioned on the value of $\boldsymbol{f}$ and on the measurement record $\boldsymbol{q}$ and, hence, the classical and quantum degrees of freedom become correlated. While the full state $\hat{\tilde{\rho}}$ is renormalized after each measurement, the measurement backaction leads to a formal redistribution of norm among the individual $\hat{\rho}_{\boldsymbol{f}}$ and hence the classical probability densities. This occurs in a manner fully equivalent with Bayes' rule, see the Appendix, so that outcomes that occur with higher (lower) probability for given values of $\boldsymbol{f}$, cause an increase (decrease) in the corresponding state components and hence the inferred likelihood for these values.

2. Gaussian states

While the augmented quantum state description of classical and quantum variables can in principle be employed with general interactions by the parallel solution of stochastic master equations for each hypothetical value of the unknown classical variable [28,29,33], the Gaussian description of both the quantum systems and the unknown classical perturbations, permits an almost straightforward application of the mean value and covariance matrix formalism to the estimation of $\boldsymbol{f}$.

[2] In the continuous variable position representation,

$$\hat{\rho}_{\boldsymbol{f}} = \int d\boldsymbol{x} d\boldsymbol{x}'\, \rho_{\boldsymbol{f}}^{\boldsymbol{x}\boldsymbol{x}'} |\boldsymbol{x}\rangle\langle\boldsymbol{x}'|.$$

To admit the unknown classical perturbations into the quantum Wigner function description we introduce an effective Gaussian Wigner function in the form of Eq. (7), $\mathcal{W}_{\hat{\rho}}^{\tilde{\boldsymbol{m}},\tilde{\boldsymbol{\Gamma}}}(\tilde{\boldsymbol{y}})$ with

$$\tilde{\boldsymbol{y}} = \begin{pmatrix} \boldsymbol{y} \\ \boldsymbol{f} \end{pmatrix}.$$

(For a discussion of how this function is consistent with the full Wigner function representation see the Appendix.) The probability densities for the classical variables,

$$P(f_j) = \int d\boldsymbol{x} d\boldsymbol{p} d\boldsymbol{f}_{i\neq j}\, \mathcal{W}_{\hat{\rho}}^{\tilde{\boldsymbol{m}},\tilde{\boldsymbol{\Gamma}}}(\boldsymbol{y},\boldsymbol{f}), \tag{24}$$

are fully characterized by the corresponding elements in the mean vector $\tilde{\boldsymbol{m}}$ and covariance matrix $\tilde{\boldsymbol{\Gamma}}$, cf. Eq. (10).

The first and second moments of the ancillary and the genuine quantum observables are in each time step first propagated similarly to Eqs. (13):

$$\tilde{\boldsymbol{m}}(t+\delta t) = \tilde{\boldsymbol{D}}_{\delta t}\tilde{\boldsymbol{S}}_{\delta t}\tilde{\boldsymbol{m}}(t), \tag{25a}$$

$$\tilde{\boldsymbol{\Gamma}}(t+\delta t) = \tilde{\boldsymbol{D}}_{\delta t}\tilde{\boldsymbol{S}}_{\delta t}\tilde{\boldsymbol{\Gamma}}(t)\tilde{\boldsymbol{S}}_{\delta t}^{T}\tilde{\boldsymbol{D}}_{\delta t}^{T} + \tilde{\boldsymbol{L}}_{\delta t}, \tag{25b}$$

where the matrix $\tilde{\boldsymbol{S}}_{\delta t}$ incorporates the displacement of the oscillator observables due to the unknown perturbations. Note that we now incorporate explicit damping and diffusion terms via the matrices $\tilde{\boldsymbol{D}}_{\delta t}$ and $\tilde{\boldsymbol{L}}_{\delta t}$ as alluded to after Eqs. (13). These are introduced, in particular, to represent the OU damping rates and diffusion constants specified in Eq. (20), see Sec. IV A for the explicit matrices relevant to the setup in Fig. 1.

The homodyne measurements with the field probe eliminate the field quantum variables $\boldsymbol{y}_B$ and update the state of the remaining degrees of freedom according to the description offered in Sec. II D, while using the augmented quantities $\tilde{\boldsymbol{a}}$, $\tilde{\boldsymbol{A}}$, and $\tilde{\boldsymbol{C}}$ in

$$\tilde{\boldsymbol{m}} = \begin{pmatrix} \tilde{\boldsymbol{a}} \\ \boldsymbol{b} \end{pmatrix}$$

and

$$\tilde{\boldsymbol{\Gamma}} = \begin{pmatrix} \tilde{\boldsymbol{A}} & \tilde{\boldsymbol{C}} \\ \tilde{\boldsymbol{C}}^{T} & \boldsymbol{B} \end{pmatrix},$$

simultaneously represent the variables

$$\hat{\tilde{\boldsymbol{y}}}_A = \begin{pmatrix} \hat{\boldsymbol{y}}_A \\ \hat{\boldsymbol{f}} \end{pmatrix}$$

of the oscillators and the unknown perturbations $\hat{\boldsymbol{f}}$. The probe field variables $\hat{\boldsymbol{y}}_B$ retain their properties and dynamics and can be eliminated, which leads to effective equations of the form of (15) for the augmented mean vector $\tilde{\boldsymbol{a}}$ and covariance matrix $\tilde{\boldsymbol{A}}$. These objects explicitly provide the estimated value of $\hat{\boldsymbol{f}}$ and the variance of the estimate around the true value.

Our equations for $\tilde{\boldsymbol{a}}$ and $\tilde{\boldsymbol{A}}$ are equivalent to classical Kalman filter theory [22], which was applied for magnetic-field sensing by continuous QND probing of an atomic collective spin in Ref. [34], see also Refs. [35–37]. Our derivation of these equations from the "quantized" form of the unknown classical parameters provides a robust starting point to explore the sensitivity limits imposed by quantum-mechanical uncertainty relations and measurement backaction on the quantum meter system in more complex settings, see also Ref. [38].

Algorithm 1. Simulation of perturbations and measurement data.

1. Numerically generate a particular classical realization of each perturbation $f_i(t)$ according to Eq. (20).
2. Simulate the conditional dynamics for $\boldsymbol{a}(t)$ and $\boldsymbol{A}(t)$ of Sec. II D using $f_i(t)$ and store the detection record $\boldsymbol{q}_B^{\text{meas}}(t)$ from the numerical sampling procedure according to Eqs. (17).

Our analysis is developed for application with measurement data obtained in an experiment, but here we synthesize such data by the Algorithm 1 and subsequently we estimate the perturbation according to Algorithm 2.

B. Smoothing

Algorithm 2 gives an estimate for the perturbations at time t conditioned upon all measurements until t. Alternatively one might attempt to provide an estimate at time t conditioned upon all measurements until and after t. That is, given the time horizon $\mathcal{H} = [0, T]$ of the complete experiment, how can we benefit from *all* measurements until time T to retrodict the strength of the perturbations at any intermediate time $t \in \mathcal{H}$?

In classical estimation theory this question is answered by so-called smoothing filters, such as the forward-backward or α/β filters for estimation of hidden Markov models [39], and the Mayne-Fraser-Potter two-filter smoother for Gaussian distributions [23,24]. Quantum equivalents of these filters were first developed by Tsang in Refs. [19–21], and following the previous sections, we present a self-contained derivation with reference to quantum measurement theory and the past quantum state (PQS) retrodiction formalism [40]. We shall apply smoothing to obtain the maximum achievable information from the "negative mass" detection scheme in Fig. 1.

1. The past quantum state

The PQS theory is a generalization of the two-state formalism by Watanabe [41] and Aharonov *et al.* [42,43] which was further developed in Ref. [40] to retrodict the outcome probabilities for the unknown outcomes of past measurements on open and monitored quantum systems. Applying the PQS theory to our "quantized" unknown classical variables $\boldsymbol{f}$, it becomes the Bayesian estimate of their values at time t, conditioned on all measurements, prior and posterior to t. We shall briefly recall the derivation of the past quantum state at the level of Hilbert-space operators before moving to the

Algorithm 2. Estimation of perturbations (filtering).

1. Acquire a detection record, either from an experiment or from a simulation by Algorithm 1.
2. Use the acquired detection record to simulate the conditional dynamics for the augmented mean values $\tilde{\boldsymbol{a}}(t)$ and covariance matrix $\tilde{\boldsymbol{A}}(t)$. Definite elements of these quantities provide the estimates of $f_i(t)$ and their variances.

convenient Gaussian Wigner function representation of states and operators.

The conditional dynamics due to the continuous monitoring of a quantum system up until time $t = n\delta t$ is described by the unnormalized density matrix following application of a sequence of operators

$$\hat{\rho}(t) = \hat{\Omega}_{\boldsymbol{q}_n} \cdots \hat{\Omega}_{\boldsymbol{q}_1} \hat{\rho}(0) \hat{\Omega}^\dagger_{\boldsymbol{q}_1} \cdots \hat{\Omega}^\dagger_{\boldsymbol{q}_n}. \tag{26}$$

Here, we assume for simplicity of notation that the system is subject to deterministic, unitary evolution and measurements with a sequence of outcome values $\boldsymbol{q}_i$ (17), so that for each time interval the evolution is governed by a unitary operator $\hat{U}$ and backaction governed by POVM operators $\hat{M}_{\boldsymbol{q}_i}$ [44], and $\hat{\Omega}_{\boldsymbol{q}_i} = \hat{M}_{\boldsymbol{q}_i}\hat{U}$. In our setting, the projective measurements of a quadrature component of the probe field segments are dominated by their Gaussian fluctuations and cause minute stochastic changes of the state of the observed oscillators, represented by the operators $\hat{M}_{\boldsymbol{q}_i} = \hat{M}_{(q_{n_B})_i} \cdots \hat{M}_{(q_1)_i}$. The POVM operators are normalized as $\int \hat{M}^\dagger_{\boldsymbol{q}} \hat{M}_{\boldsymbol{q}}\, d\boldsymbol{q} = \hat{\mathbb{1}}$, and according to quantum measurement theory, the trace norm of (26) yields the joint probability of all the specified outcome results.

Proceeding with a projective measurement $\hat{\Pi}_{y_j} = \hat{\Pi}^\dagger_{y_j} = |y_j\rangle\langle y_j|$ at t on the observed quantum system, followed by continued optical probing until $T = N\delta t$ yields the conditioned state

$$\hat{\rho}(T) = \hat{\Omega}_{\boldsymbol{q}_N} \cdots \hat{\Omega}_{\boldsymbol{q}_{n+1}} \hat{\Pi}_{y_j} \hat{\rho}(t) \hat{\Pi}^\dagger_{y_j} \hat{\Omega}^\dagger_{\boldsymbol{q}_{n+1}} \cdots \hat{\Omega}^\dagger_{\boldsymbol{q}_N}, \tag{27}$$

and the joint probability density for the full optical detection record $\boldsymbol{q}_1, \ldots, \boldsymbol{q}_N$ *and* the projective outcome value y_j at time t is given by

$$\begin{aligned} P(\boldsymbol{q}_1, \ldots, y_j, \ldots \boldsymbol{q}_N) &= \mathrm{tr}[\hat{\rho}(T)] \\ &= \mathrm{tr}\big[\hat{\Omega}_{\boldsymbol{q}_N} \cdots \hat{\Omega}_{\boldsymbol{q}_{n+1}} \hat{\Pi}_{y_j} \hat{\rho}(t) \hat{\Pi}^\dagger_{y_j} \hat{\Omega}^\dagger_{\boldsymbol{q}_{n+1}} \cdots \hat{\Omega}^\dagger_{\boldsymbol{q}_N}\big] \\ &\equiv \mathrm{tr}\big[\hat{\Pi}_{y_j} \hat{\rho}(t) \hat{\Pi}^\dagger_{y_j} \hat{E}(t)\big], \end{aligned} \tag{28}$$

where we used the cyclic property of the trace to define the so-called *measurement effect operator* on the same Hilbert space as $\hat{\rho}$,

$$\hat{E}(t) = \hat{\Omega}^\dagger_{\boldsymbol{q}_{n+1}} \cdots \hat{\Omega}^\dagger_{\boldsymbol{q}_N} \hat{\mathbb{1}} \hat{\Omega}_{\boldsymbol{q}_N} \cdots \hat{\Omega}_{\boldsymbol{q}_{n+1}}. \tag{29}$$

The expression for $\hat{E}(t)$ is similar to the expression for the time-evolved density matrix, except the operator $\hat{E}(t)$ is conditioned on the detection record for times after t and is found by a sequential backward evolution from the final value, $\hat{E}(T) = \hat{\mathbb{1}}$ by the adjoint of the POVM operators. For generalization to cases including damping and dissipation, see Ref. [40].

After all the field measurements have been done, the value of the joint probability distribution (28) evaluated at the fixed entries of the detection record yields the (conditional) probability for the still unknown outcome y_j. Conditioned on only measurements until time t, and on measurements before and after time t, this yields

$$P(y_j|\boldsymbol{q}_1 \cdots \boldsymbol{q}_n) \propto \mathrm{tr}\big[\hat{\Pi}_{y_j} \hat{\rho}(t)\big], \tag{30a}$$

$$P_{\mathrm{pqs}}(y_j|\boldsymbol{q}_1 \cdots \boldsymbol{q}_N) \propto \mathrm{tr}\big[\hat{\Pi}_{y_j} \hat{\rho}(t) \hat{\Pi}^\dagger_{y_j} \hat{E}(t)\big], \tag{30b}$$

respectively, where the probabilities are normalized by the sum (or integral) of the expressions over the argument y_j.

The first expression is the usual Born rule, and it applies also when $\hat{\Pi}_{y_j}$ represents the unknown classical perturbations, in which case the conditional quantum state $\hat{\rho}(t)$ acts as a Bayesian *filter*. The second expression retrodicts past measurement outcome probabilities [40], and the pair of operators $\hat{\rho}(t)$ and $\hat{E}(t)$ corresponds to a Bayesian *two-way smoothing filter* for the past value of the unknown classical perturbations [19,20].

2. Gaussian states

To apply the Gaussian state formalism, we represent the augmented operator $\hat{\tilde{E}}(t)$ in a manner similar to Eq. (21) for $\hat{\tilde{\rho}}$,[3]

$$\hat{\tilde{E}} = \int d\boldsymbol{f}\, |\boldsymbol{f}\rangle\langle\boldsymbol{f}| \otimes \hat{E}_{\boldsymbol{f}}. \tag{31}$$

Both $\hat{\tilde{\rho}}$ and $\hat{\tilde{E}}$ are operators on the reduced Hilbert space of the oscillators and perturbations, described by variables

$$\hat{\tilde{\boldsymbol{y}}}_A = \begin{pmatrix} \hat{\boldsymbol{y}}_A \\ \hat{\boldsymbol{f}} \end{pmatrix},$$

and they are evolved with Gaussian Wigner representations $\mathcal{W}^{\tilde{\boldsymbol{a}}_\rho, \tilde{\boldsymbol{A}}_\rho}_{\hat{\tilde{\rho}}}(\tilde{\boldsymbol{y}}_A)$ and $\mathcal{W}^{\tilde{\boldsymbol{a}}_E, \tilde{\boldsymbol{A}}_E}_{\hat{\tilde{E}}}(\tilde{\boldsymbol{y}}_A)$ which are fully determined by the first and second moments $\tilde{\boldsymbol{A}}_\rho, \tilde{\boldsymbol{a}}_\rho$ and $\tilde{\boldsymbol{A}}_E, \tilde{\boldsymbol{a}}_E$. The moments $\tilde{\boldsymbol{A}}_\rho$, $\tilde{\boldsymbol{a}}_\rho$ evolve according to the theory presented in the previous section and are now explicitly labeled with the index ρ while first and second moments determined by the measurement effect operator follow a backward time evolution. For the evolution in each time step including the field segments, we have

$$\tilde{\boldsymbol{m}}_E(t - \delta t) = \tilde{\boldsymbol{D}}^-_{\delta t} \tilde{\boldsymbol{S}}^-_{\delta t} \tilde{\boldsymbol{m}}_E(t), \tag{32a}$$

$$\tilde{\boldsymbol{\Gamma}}_E(t - \delta t) = \tilde{\boldsymbol{D}}^-_{\delta t} \tilde{\boldsymbol{S}}^-_{\delta t} \tilde{\boldsymbol{\Gamma}}_E(t) \tilde{\boldsymbol{S}}^{-T}_{\delta t} \tilde{\boldsymbol{D}}^{-T}_{\delta t} + \tilde{\boldsymbol{L}}^-_{\delta t}. \tag{32b}$$

The elements of $\tilde{\boldsymbol{S}}^-_{\delta t}$ follow from the equation of motion $\hat{y}_i(t - \delta t) \approx \hat{y}_i(t) - \hat{y}_i(t)\delta t$, while the damping and diffusion terms in the backwards equations have to be derived by an analysis of their physical origin. When "played in reverse," the classical OU process experiences negative damping but unchanged stochastic fluctuations. For the specific situation described by the setup in Fig. 1, we incorporate the parameters of the OU process in the matrix $\tilde{\boldsymbol{D}}^-_{\delta t}$ by negating the γ_i term in $\tilde{\boldsymbol{D}}_{\delta t}$ while the diffusion rates σ_i are unchanged and $\tilde{\boldsymbol{L}}^-_{\delta t} = \tilde{\boldsymbol{L}}_{\delta t}$ (see details in Sec. IV A).

The monitoring of the field components leads to a stochastic sequence of POVM operators, which shall be applied in reverse to yield $\hat{\tilde{E}}$. The effective measurement updates of

[3] In the continuous basis,

$$\hat{\tilde{E}} = \int d\boldsymbol{x} d\boldsymbol{x}' d\boldsymbol{f}\, \tilde{E}^{\boldsymbol{x}\boldsymbol{x}'}_{\boldsymbol{f}} |\boldsymbol{f}\rangle\langle\boldsymbol{f}| \otimes |\boldsymbol{x}\rangle\langle\boldsymbol{x}'|.$$

$\tilde{\boldsymbol{a}}_E(t)$ and $\tilde{\boldsymbol{A}}_E(T)$ governed by the detection record $\boldsymbol{q}_B^{\rm meas}(t)$ are thus on the same form as Eq. (15). The Wigner function for $\hat{E}(T) = \hat{\mathbb{1}}$ is a uniform Gaussian distribution (the constant function with infinite variance) on the oscillators and classically unknown parameters. In practice we assume vanishing mean values and $\tilde{\boldsymbol{A}}_E(T) = \mathrm{diag}(\ldots, v, \ldots)$ with a suitably large dimensionless $v = 10^4$ at $t = T$, and we have verified that the backward-evolved first and second moments quickly become independent of these values.

Rather than explicitly reconstructing the operators $\hat{\tilde{\rho}}$ and $\hat{\tilde{E}}$, it is much more convenient for our purpose to refer to their first and second moments and their corresponding Gaussian Wigner functions. This is because the trace of a product of two operators equals the integral of the product of their Wigner functions (4), and the PQS expression, $P_{\rm pqs}(f_j') \propto \mathrm{tr}[(|f_j'\rangle\langle f_j'|\hat{\tilde{\rho}})(|f_j'\rangle\langle f_j'|\hat{\tilde{E}})]$ for the variable $y_j \to f_j'$ in Eq. (30b) involves such a product of operators $|f_j'\rangle\langle f_j'|\hat{\tilde{X}}$, with $X = \rho, E$.

Multiplication of $\hat{\tilde{\rho}}$ and $\hat{\tilde{E}}$ by the projection operator yields the transformed Wigner function, see the Appendix,

$$\mathcal{W}_{|f_j'\rangle\langle f_j'|\hat{\tilde{X}}}(\tilde{\boldsymbol{y}}_A) = \delta(f_j - f_j')\mathcal{W}_{\hat{\tilde{X}}}(\tilde{\boldsymbol{y}}_A), \tag{33}$$

and the PQS probability density for f_j' in Eq. (30b) can be directly written in terms of the Gaussian Wigner functions,

$$\begin{aligned} P_{\rm pqs}(f_j') &\propto \mathrm{tr}[(|f_j'\rangle\langle f_j'|\hat{\tilde{\rho}})(|f_j'\rangle\langle f_j'|\hat{\tilde{E}})] \\ &\propto \int d\boldsymbol{x}_A d\boldsymbol{p}_A d\boldsymbol{f}\ \mathcal{W}_{|f_j'\rangle\langle f_j'|\hat{\tilde{\rho}}} \times \mathcal{W}_{|f_j'\rangle\langle f_j'|\hat{\tilde{E}}} \\ &= \int d\boldsymbol{x}_A d\boldsymbol{p}_A d\boldsymbol{f}_{i\neq j} \left(\mathcal{W}_{\hat{\tilde{\rho}}}^{\tilde{\boldsymbol{a}}_\rho, \tilde{\boldsymbol{A}}_\rho} \times \mathcal{W}_{\hat{\tilde{E}}}^{\tilde{\boldsymbol{a}}_E, \tilde{\boldsymbol{A}}_E}\right)\Big|_{f_j = f_j'} \\ &= \int d\boldsymbol{x}_A d\boldsymbol{p}_A d\boldsymbol{f}_{i\neq j}\ \mathcal{W}_{\hat{\tilde{\rho}},\hat{\tilde{E}}}^{\tilde{\boldsymbol{a}}_{\rho,E}, \tilde{\boldsymbol{A}}_{\rho,E}}(\boldsymbol{y}_A, \boldsymbol{f}_{i\neq j}, f_j'). \end{aligned} \tag{34}$$

The integrals in the last two lines are over all variables $\tilde{\boldsymbol{y}}_A$ except the desired value of the argument f_j'. In the last expression we have used that the product of two multivariate Gaussian functions is also a multivariate Gaussian function, with the covariance matrix and mean values given by

$$\tilde{\boldsymbol{A}}_{\rho,E}^{-1} = \tilde{\boldsymbol{A}}_\rho^{-1} + \tilde{\boldsymbol{A}}_E^{-1}, \tag{35a}$$

$$\tilde{\boldsymbol{a}}_{\rho,E} = \tilde{\boldsymbol{A}}_{\rho,E}\left(\tilde{\boldsymbol{A}}_\rho^{-1}\tilde{\boldsymbol{a}}_\rho + \tilde{\boldsymbol{A}}_E^{-1}\tilde{\boldsymbol{a}}_E\right). \tag{35b}$$

These expressions directly yield the retrodicted (smoothed) estimate of the time-dependent perturbations and their accompanying variances based on the entire detection record. The implementation of the formalism is summarized in Algorithm 3.

IV. NUMERICAL EXAMPLES

We have presented a general, compact mathematical formalism for the Gaussian quantum states and estimates of classical parameters conditioned on continuous quadrature (homodyne) measurements on probe fields. We shall now demonstrate numerical application of the formalism and evaluate the assessment of the probing scenario illustrated in Fig. 1 and described by Eq. (1). The entanglement and noise cancellation properties of the scheme have been analyzed and experimentally demonstrated in the frequency domain [45], i.e., noise power spectra of the probe signal measurements have been compared and agree with theory. Here, we shall address the explicit time domain analysis, and provide the time-dependent estimator and compare it with its true value in simulated experiments.

Algorithm 3. Estimation of the perturbations by smoothing.

1. Obtain data record from experiments or by simulation with Algorithm 1.
2. Apply Algorithm 2 to obtain the conditional dynamics for $\tilde{\boldsymbol{a}}_\rho(t)$ and $\tilde{\boldsymbol{A}}_\rho(t)$.
3. Use the same measured or simulated detection records to obtain the backward conditional dynamics for $\tilde{\boldsymbol{a}}_E(t)$ and $\tilde{\boldsymbol{A}}_E(t)$.
4. Calculate the retrodicted PQS moments $\tilde{\boldsymbol{a}}_{\rho,E}(t)$ and $\tilde{\boldsymbol{A}}_{\rho,E}(t)$ in Eq. (35). Definite elements of these quantities provide the smoothed, PQS estimates of $f_i(t)$ and their variances.

A. Physical parameters

We assume the Hamiltonian in Eq. (1), describing how the oscillator variables $\hat{\boldsymbol{y}}_A = (\hat{x}_{S_1}, \hat{p}_{S_1}, \hat{x}_{S_2}, \hat{p}_{S_2})$ interact sequentially with the field variables of the consecutive light segments $\hat{\boldsymbol{y}}_B = (\hat{x}_{L_1}, \hat{p}_{L_1}, \hat{x}_{L_2}, \hat{p}_{L_2})$.

By assuming fewer degrees of freedom and vanishing values of some of the interaction parameters in Eq. (1) we can use the same theoretical model to study the estimation of single or multiple perturbations, by a single probe beam or two probe beams and a single or oscillator mode two oscillator modes. We can thus directly observe how the backaction-evading mechanism affects the dynamics of the physical systems and the estimation of the perturbations.

We henceforth assume for convenience that all physical parameters are given in units of the values listed in Table I applicable, e.g., to the probing of ensemble atomic spins, subject to magnetic-field fluctuations [35,46]. The matrix and vector quantities applied in our formalism are listed in the following equations, where the vector and matrix elements refer to the physical observables and classical noise in the

TABLE I. Parameter values used, if not set to zero, in the numerical simulations ($i, j = 1, 2$). These values may for example represent vector magnetometry with atomic spin ensembles.

Parameter	Value
Time step	$\delta t = 10^{-5}$–10^{-7} s
Oscillation frequencies	$\lvert\omega_i\rvert = 0.1 \times 2\pi/\mathrm{ms} \approx 0.63$ kHz
Light couplings	$\lvert\kappa_{i,j}\rvert = 135$ Hz
Classical field couplings	$c_x = c_p = 1.5 \times 10^4$ Hz
OU damping rate of f_x	$\gamma_x = 100$ Hz
OU diffusion rate of f_x	$\sigma_x = 10$ Hz
OU damping rate of f_p	$\gamma_p = 10$ Hz
OU diffusion rate of f_p	$\sigma_p = 1$ Hz

following order $(\hat{x}_{S_1}, \hat{p}_{S_1}, \hat{x}_{S_2}, \hat{p}_{S_2}, f_x, f_p, \hat{x}_{L_1}, \hat{p}_{L_1}, \hat{x}_{L_2}, \hat{p}_{L_2})$:

$$\tilde{\boldsymbol{S}}_{\delta t} = \begin{pmatrix} \cos\omega_1\delta t & \sin\omega_1\delta t & 0 & 0 & c_x\delta t & 0 & 0 & \kappa_{1,1}\sqrt{\delta t} & 0 & 0 \\ -\sin\omega_1\delta t & \cos\omega_1\delta t & 0 & 0 & 0 & c_p\delta t & 0 & 0 & -\kappa_{1,2}\sqrt{\delta t} & 0 \\ 0 & 0 & \cos\omega_2\delta t & \sin\omega_2\delta t & 0 & 0 & 0 & \kappa_{2,1}\sqrt{\delta t} & 0 & 0 \\ 0 & 0 & -\sin\omega_2\delta t & \cos\omega_2\delta t & 0 & 0 & 0 & 0 & -\kappa_{2,2}\sqrt{\delta t} & 0 \\ 0 & 0 & 0 & 0 & 1 & 0 & 0 & 0 & 0 & 0 \\ 0 & 0 & 0 & 0 & 0 & 1 & 0 & 0 & 0 & 0 \\ 0 & \kappa_{1,1}\sqrt{\delta t} & 0 & \kappa_{2,1}\sqrt{\delta t} & 0 & 0 & 1 & 0 & 0 & 0 \\ 0 & 0 & 0 & 0 & 0 & 0 & 0 & 1 & 0 & 0 \\ 0 & 0 & 0 & 0 & 0 & 0 & 0 & 0 & 1 & 0 \\ -\kappa_{1,2}\sqrt{\delta t} & 0 & -\kappa_{2,2}\sqrt{\delta t} & 0 & 0 & 0 & 0 & 0 & 0 & 1 \end{pmatrix}, \tag{36}$$

$$\tilde{\boldsymbol{D}}_{\delta t} = \mathrm{diag}(1, 1, 1, 1, (1-\gamma_x\delta t), (1-\gamma_p\delta t), 1, 1, 1, 1), \tag{37}$$

$$\tilde{\boldsymbol{L}}_{\delta t} = \mathrm{diag}(0, 0, 0, 0, 2\sigma_x\delta t, 2\sigma_p\delta t, 0, 0, 0, 0), \tag{38}$$

$$\boldsymbol{F}_{\delta t} = (c_x f_x\delta t, c_p f_p\delta t, 0, 0, 0, 0, 0, 0)^T, \tag{39}$$

$$\boldsymbol{\Pi} = \boldsymbol{\pi}_{L_1} \oplus \boldsymbol{\pi}_{L_2} = \boldsymbol{\pi}_x \oplus \boldsymbol{\pi}_p = \mathrm{diag}(1, 0, 0, 1), \tag{40}$$

$$\boldsymbol{\Delta}_B^{\mathrm{meas}} = \mathrm{diag}\big(\Delta_{L_1}, 0, 0, \Delta_{L_2}\big) \equiv \mathrm{diag}\big(x_{L_1}^{\mathrm{meas}} - \langle\hat{x}_{L_1}\rangle, 0, 0, p_{L_2}^{\mathrm{meas}} - \langle\hat{p}_{L_2}\rangle\big), \tag{41}$$

When the classical perturbations have known values, they displace the quadrature observables

$$\hat{\boldsymbol{y}} = \begin{pmatrix} \hat{\boldsymbol{y}}_A \\ \hat{\boldsymbol{y}}_B \end{pmatrix}$$

by the argument $\boldsymbol{F}_{\delta t}$ in Eq. (39), and the interaction matrix $\boldsymbol{S}_{\delta t}$ for the quantum variables is given for small values of δt by omitting the f_x and f_p rows and columns (5 and 6) in $\tilde{\boldsymbol{S}}_{\delta t}$ in Eq. (36). When the perturbing fields are instead represented as ancillary quantum variables, i.e., $f_i \to \hat{f}_i$ in $\hat{H}$, the augmented system variables are

$$\hat{\tilde{\boldsymbol{y}}} = \begin{pmatrix} \hat{\tilde{\boldsymbol{y}}}_A \\ \hat{\boldsymbol{y}}_B \end{pmatrix} \quad \text{where} \quad \hat{\tilde{\boldsymbol{y}}}_A = \begin{pmatrix} \hat{\boldsymbol{y}}_A \\ \hat{f}_x \\ \hat{f}_p \end{pmatrix},$$

and the full $\tilde{\boldsymbol{S}}_{\delta t}$ matrix and OU dissipation $\tilde{\boldsymbol{D}}_{\delta t}$ in Eq. (37), and OU diffusion $\tilde{\boldsymbol{L}}_{\delta t}$ in Eq. (38) are used.

Rather than extensively scoping out the dependence of the results on different combinations of physical parameters, we focus our numerical efforts on highlighting the behavior with few fixed parameter settings, specified by the values in Table I, and observing how the switching on and off of different terms change the sensing mechanisms and hence performance.

B. Monitoring of unperturbed oscillators

In this section we consider scenarios where the classical perturbations are absent $f_x(t) = f_p(t) = 0$ or, equivalently, $c_x = c_p = 0$.

1. *Probing of a single oscillator*

Consider a single mode

$$\hat{\boldsymbol{y}} = \begin{pmatrix} \hat{x} \\ \hat{p} \end{pmatrix}$$

with dimensionless canonical variables $[\hat{x}, \hat{p}] = i$ with $\Delta\hat{x}^2\Delta\hat{p}^2 \geqslant 1/4$,[4] subject to the harmonic-oscillator Hamiltonian with corresponding Heisenberg time evolution

$$\hat{H}_\omega = \frac{\hbar\omega}{2}(\hat{x}^2 + \hat{p}^2), \tag{42a}$$

$$\hat{x}(t) = \hat{x}(0)\cos\omega t + \hat{p}(0)\sin\omega t, \tag{42b}$$

$$\hat{p}(t) = \hat{p}(0)\cos\omega t - \hat{x}(0)\sin\omega t. \tag{42c}$$

In suitable interaction pictures (rotating frames), systems may be described by positive, negative, and vanishing values of $\omega = 0$ in (42). The backaction from a precise measurement of $\hat{x}$ at $t = 0$ squeezes the variance $\Delta\hat{x}(0)^2 \to 0$ and induces a corresponding antisqueezing $\Delta\hat{p}(0)^2 \to \infty$. For $\omega \neq 0$, the reduced and increased variances will then oscillate back and forth between the two operators as their time evolution amounts to rotation about the origin in phase space with angular frequency ω, as shown in Fig. 3(a).

Rather than such an abrupt measurement and preparation of a squeezed state, we consider continuous probing by the sequential interaction with infinitesimal segments of a laser probe beam with quantum degrees of freedom $\hat{\boldsymbol{y}}_B = (\hat{x}_L, \hat{p}_L)^T$ subject to a subsequent measurement. Specifically, an interac-

[4]For a mechanical oscillator $\hat{H}_\omega = \frac{p_{\mathrm{mech}}^2}{2m} + \frac{1}{2}m\omega^2 x_{\mathrm{mech}}^2$ with mass m the dimensionless variables are given by $\hat{x} = \hat{x}_{\mathrm{mech}}/x_0$ and $\hat{p} = \hat{p}_{\mathrm{mech}}x_0/\hbar$, where $x_0^2 = \hbar/(m\omega)$.

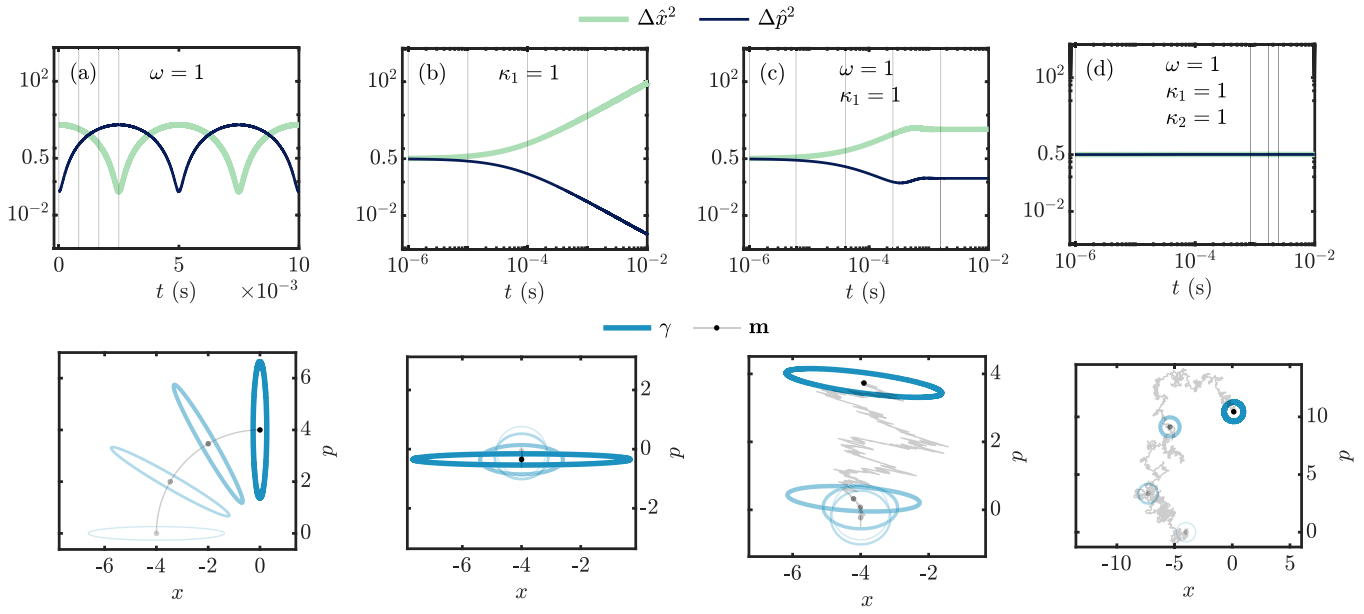

FIG. 3. Evolution of a single oscillator. Numerical examples for different scenarios (columns) with nonzero parameter values from Table I. (a) Squeezed state oscillating without measurements. (b) Coherent state squeezed by continuous optical measurements sensitive to the oscillator quadrature $\hat{p}$. (c) Same as panel (b) but including oscillations. (d) Same as panel (c) but including continuous optical measurements sensitive to the oscillator quadrature $\hat{x}$. Variances are shown as function of time in the upper panels. Snapshots of associated Wigner function contour lines are shown in the lower panels around the time-dependent mean values (translucent gray solid line), as in Fig. 2. The snapshot times are indicated by vertical lines in the upper panels and their sequence is indicated by increasing linewidth and opacity.

tion with $\hat{p}_L$ and measurement of $\hat{x}_L$,

$$\hat{H}^p_\kappa = \hbar\kappa\,\hat{p}_S\hat{p}_L, \quad \boldsymbol{\pi}_1 = \boldsymbol{\pi}_x, \tag{43}$$

results in a small incremental squeezing of $\hat{p}_S$ and antisqueezing of $\hat{x}_S$ while

$$\hat{H}^x_\kappa = \hbar\kappa\,\hat{x}_S\hat{x}_L, \quad \boldsymbol{\pi}_1 = \boldsymbol{\pi}_p, \tag{44}$$

results in a small incremental squeezing of $\hat{x}_S$ and antisqueezing of $\hat{p}_S$. This leads to the following distinct scenarios and accumulated effects on the oscillator.

Single probe, $\omega = 0$—squeezing accumulates with a variance scaling asymptotically as $1/t$ [Fig. 3(b)]. For an analytical derivation of this result, see, e.g., Ref. [38].

Single probe, $\omega \neq 0$—squeezing is partially counteracted by the rotation and the variances become asymptotically constant [Fig. 3(c)].

Two probes, $\omega = 0$ *or* $\omega \neq 0$—two light modes $\hat{\boldsymbol{y}}_B = (\hat{x}_{L_1}, \hat{p}_{L_1}, \hat{x}_{L_2}, \hat{p}_{L_2})^T$ interacting with different quadratures

$$\hat{H}_{\kappa_1,\kappa_2} = \hat{H}^p_{\kappa_1} + \hat{H}^x_{\kappa_2}, \quad \begin{matrix}\boldsymbol{\pi}_1 = \boldsymbol{\pi}_x \\ \boldsymbol{\pi}_2 = \boldsymbol{\pi}_p,\end{matrix} \tag{45}$$

the squeezing effects compete, and for $\kappa_1 = \kappa_2$ no net squeezing occurs [Fig. 3(d)].

2. *Probing of two oscillators—EPR variables*

Consider now a two-mode system $\hat{\boldsymbol{y}}_A = (\hat{x}_{S_1}, \hat{p}_{S_1}, \hat{x}_{S_2}, \hat{p}_{S_2})^T$ with $[\hat{x}_{S_i}, \hat{p}_{S_j}] = i\delta_{i,j}$ for $i, j = 1, 2$ and a separable oscillator Hamiltonian

$$\hat{H}_{\omega_1,\omega_2} = \hat{H}_{\omega_1} + \hat{H}_{\omega_2}. \tag{46}$$

Precise knowledge of both quadratures for the individual oscillators is prohibited by the Heisenberg uncertainty relation, yet we can define four new EPR-type position and momentum variables [13],

$$\hat{\boldsymbol{y}}^\pm_A \equiv \begin{pmatrix}\hat{x}_- \\ \hat{p}_+ \\ \hat{x}_+ \\ \hat{p}_-\end{pmatrix} \equiv \frac{1}{\sqrt{2}}\begin{pmatrix}\hat{x}_{S_1} - \hat{x}_{S_2} \\ \hat{p}_{S_1} + \hat{p}_{S_2} \\ \hat{x}_{S_1} + \hat{x}_{S_2} \\ \hat{p}_{S_1} - \hat{p}_{S_2}\end{pmatrix}, \tag{47}$$

satisfying the commutation relations

$$[\hat{x}_-, \hat{p}_+] = [\hat{x}_+, \hat{p}_-] = 0, \tag{48}$$

$$[\hat{x}_-, \hat{p}_-] = [\hat{x}_+, \hat{p}_+] = i. \tag{49}$$

Hence $\hat{x}_-$ and $\hat{p}_+$ can both be principally known to arbitrary precision, $\Delta\hat{x}^2_-\Delta\hat{p}^2_+ \geqslant 0$, while the values of the adjoint variables $\hat{x}_+$ and $\hat{p}_-$ become correspondingly uncertain. The EPR variables can be written $\hat{\boldsymbol{y}}^\pm_A = \boldsymbol{\mathcal{R}}\hat{\boldsymbol{y}}_A$ with the matrix

$$\boldsymbol{\mathcal{R}} = \frac{1}{\sqrt{2}}\begin{pmatrix}1 & 0 & -1 & 0 \\ 0 & 1 & 0 & 1 \\ 1 & 0 & 1 & 0 \\ 0 & 1 & 0 & -1\end{pmatrix}, \tag{50}$$

and their first and second moments are given by

$$\boldsymbol{a}^\pm = \boldsymbol{\mathcal{R}}\boldsymbol{a}, \quad \boldsymbol{A}^\pm = \boldsymbol{\mathcal{R}}\boldsymbol{A}\boldsymbol{\mathcal{R}}^T. \tag{51}$$

Two laser probes $\hat{\boldsymbol{y}}_B = (\hat{x}_{L_1}, \hat{p}_{L_1}, \hat{x}_{L_2}, \hat{p}_{L_2})^T$ permit simultaneous measurements of $\hat{x}_-$ and $\hat{p}_+$ if we assume the

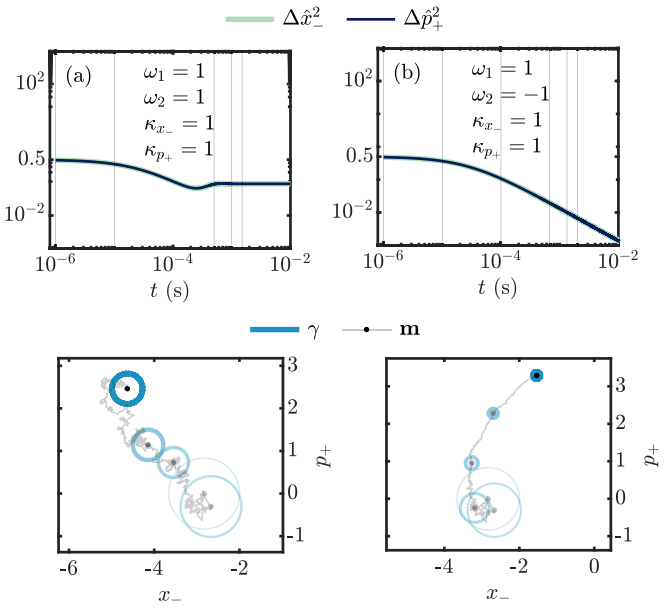

FIG. 4. Evolution of two oscillators. As Fig. 3 but for commuting EPR variables $\hat{x}_-$ and $\hat{p}_+$ continuously measured indirectly starting from an initial coherent state. The oscillator frequency ω_1 is positive and (a) ω_2 is positive or (b) ω_2 is negative. The variance reduction in panel (b) is also attained for $\omega_1 = \omega_2 = 0$.

interactions

$$\begin{aligned}\hat{H}^{p}_{\kappa_{1,1},\kappa_{2,1}} &= \hbar\big(\kappa_{1,1}\hat{p}_{S_1} + \kappa_{2,1}\hat{p}_{S_2}\big)\hat{p}_{L_1},\\ &\quad\text{(assume } \kappa_{1,1} = \kappa_{2,1} \equiv \kappa_p/\sqrt{2})\\ &= \hbar\kappa_p\hat{p}_+\hat{p}_{L_1} \equiv \hat{H}^{p_+}_{\kappa_{p_+}}, \quad \boldsymbol{\pi}_1 = \boldsymbol{\pi}_x, \end{aligned} \tag{52}$$

and

$$\begin{aligned}\hat{H}^{x}_{\kappa_{1,2},\kappa_{2,2}} &= \hbar\big(\kappa_{1,2}\hat{x}_{S_1} + \kappa_{2,2}\hat{x}_{S_2}\big)\hat{x}_{L_2},\\ &\quad\text{(assume } \kappa_{1,2} = -\kappa_{2,2} \equiv \kappa_x/\sqrt{2})\\ &= \hbar\kappa_x\hat{x}_-\hat{x}_{L_2} \equiv \hat{H}^{x_-}_{\kappa_{x_-}}, \quad \boldsymbol{\pi}_2 = \boldsymbol{\pi}_p. \end{aligned} \tag{53}$$

In summary, we have

$$\hat{H}^{p_+}_{\kappa_p} + \hat{H}^{x_-}_{\kappa_x} \equiv \hbar\kappa_p\hat{p}_+\hat{p}_{L_1} + \hbar\kappa_x\hat{x}_-\hat{x}_{L_2}, \quad \begin{matrix}\boldsymbol{\pi}_1 = \boldsymbol{\pi}_x\\ \boldsymbol{\pi}_2 = \boldsymbol{\pi}_p,\end{matrix} \tag{54}$$

which is similar to Eq. (45), but here the operators $\hat{x}_-$ and $\hat{p}_+$ commute and can be simultaneously measured and squeezed. This leads to the following distinct accomplishments.

Same sign, $\omega = \omega_1 = \omega_2$—the free evolution of the oscillators yields

$$\begin{pmatrix}\hat{x}_-(t)\\ \hat{p}_+(t)\end{pmatrix} = \begin{pmatrix}\hat{x}_-(0)\cos\omega t + \hat{p}_-(0)\sin\omega t\\ \hat{p}_+(0)\cos\omega t - \hat{x}_+(0)\sin\omega t\end{pmatrix}, \tag{55}$$

and the squeezed and antisqueezed uncertainties oscillate periodically between the $\hat{x}_-$ and $\hat{p}_-$ variables (respectively, $\hat{p}_+$ and $\hat{x}_+$), while the continuously probed system reaches a finite steady squeezing of the collective observables, see Fig. 4(a).

Opposite sign, $\omega = \omega_1 = -\omega_2$—the free evolution of the oscillators yields

$$\begin{pmatrix}\hat{x}_-(t)\\ \hat{p}_+(t)\end{pmatrix} = \begin{pmatrix}\hat{x}_-(0)\cos\omega t + \hat{p}_+(0)\sin\omega t\\ \hat{p}_+(0)\cos\omega t - \hat{x}_-(0)\sin\omega t\end{pmatrix}, \tag{56}$$

which show that the variables $\hat{x}_-$ and $\hat{p}_+$ do not couple to the antisqueezed observables and are both squeezed with variances scaling asymptotically as $1/t$, as one would conclude from Ref. [38], see Fig. 4(b).

In conclusion, by choosing appropriate probe strengths and oscillator frequencies, $\kappa_{1,1} = \kappa_{1,2} = \kappa_{2,1} = -\kappa_{2,2}$, $\omega_1 = -\omega_2$, the EPR variables $\hat{x}_-$ and $\hat{p}_+$ in Fig. 1 can both be determined to arbitrary precision with no adverse measurement backaction or coupling to their conjugate, antisqueezed observables. As proposed by Tsang and Caves [7,8] this property can be leveraged for the sensing of perturbations acting on one of the oscillators.

C. Estimation of constant perturbations

We now consider the estimation of the unknown value of constant perturbations ($\gamma_i = \sigma_i = 0$) on the oscillator system. We assume initial oscillator ground states, $a_i = 0$ and $A_{ij} = \delta_{ij}$, and perturbations governed by an initial Gaussian distribution with vanishing mean and variance of 0.05 in all our simulations.

It is possible to asymptotically approach the true values $\langle f_i\rangle \to f_i$ to an arbitrary precision by measuring for longer and longer times, but the rate at which the variance of our estimate decreases depends on the measurement scenario, as shown in Fig. 5. All parameters are given in units of the values in Table I.

For a single oscillator with $\omega_1 = 0$, subject to a single probe beam, by the analysis in Ref. [38], it is possible to asymptotically achieve $\Delta {f_p}^2 \propto 1/t^3$ for the sensing of a single unknown perturbation f_p, while we have no sensitivity to the value of f_x, see Fig. 5(a). This reflects that the number of measurements ("samples") increases linearly with time, while the measurements are performed with a progressively better (more squeezed) sensor, cf. Fig. 3(b). The right panel shows the estimated and true values of f_x and f_p (assuming very distinct true values for ease of identification).

By coupling the oscillator quadratures to two different perturbations and probe beams in Fig. 5(b), the variance on the estimator of both perturbations approach zero but at slower asymptotic rates $\Delta {f_x}^2$, $\Delta {f_p}^2 \propto 1/t$. This is because squeezing of both oscillator quadratures is prohibited by the uncertainty relation, and hence the sensor does not improve with time, cf. Fig. 3(d).

We now introduce the second oscillator. Initially assuming $\omega_1 = \omega_2 = 0$ and probing the EPR variables $\hat{x}_-$ and $\hat{p}_+$ restores the benefits of squeezing, cf. Fig. 4(b), and results in an asymptotic $\Delta {f_x}^2$, $\Delta {f_x}^2 \propto 1/t^3$ scaling for our estimate of both perturbations, as shown in Fig. 5(c). The right panel shows that the correct values of the perturbations are rapidly identified with high precision.

It is worth commenting that the solution of the nonlinear matrix Riccati equation for the covariance matrix by the decomposition as a matrix fraction $\boldsymbol{A} = \boldsymbol{W}\boldsymbol{U}^{-1}$, in simple cases leads to variances that can be expressed as a ratio between

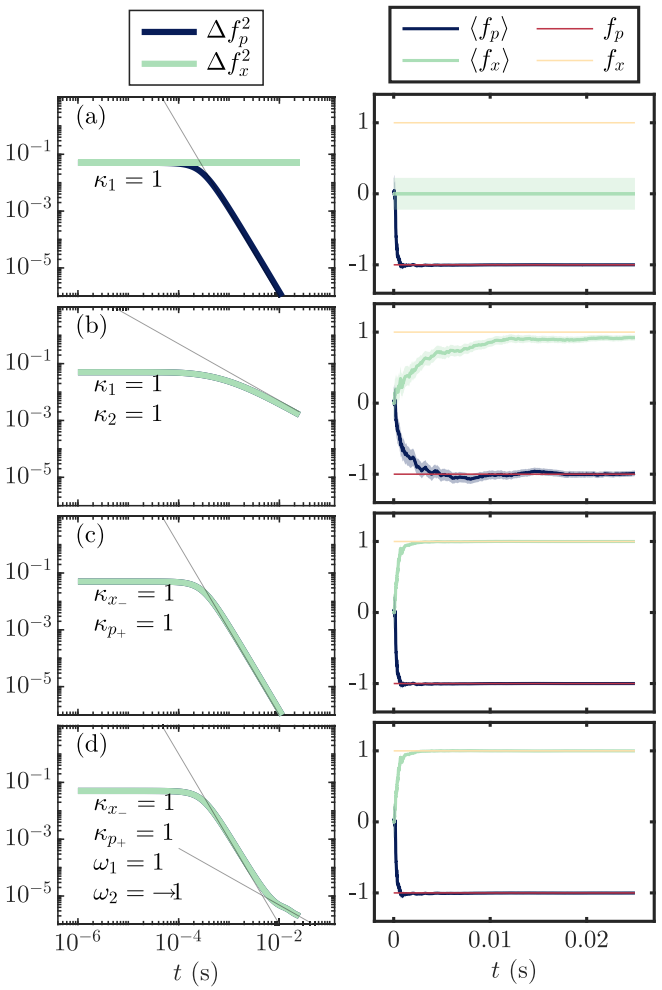

FIG. 5. Estimation of constant perturbations ($\gamma_i = \sigma_i = 0$). The left panels show the variance Δf_i^2 with $1/t$ and $1/t^3$ trend lines. The right panels show the true and estimated perturbation $\langle f_i \rangle \pm \Delta f_i$ (the true values shown by the thin lines are taken to be large positive and negative to distinguish their estimates clearly in the panels). The upper panels (a) show the results for probing of $\hat{p}_{S_1}$ for a single oscillator with $\omega_1 = 0$ being sensitive to only the value of f_p. Panels (b) show the results for probing of $\hat{x}_{S_1}$ and $\hat{p}_{S_1}$ of a single oscillator with $\omega_1 = 0$, being sensitive to both f_x and f_p, but without the benefit of squeezing of the oscillator. Panels (c) are for the probing and squeezing of EPR variables $\hat{x}_-$ and $\hat{p}_+$ of two oscillators with $\omega_1 = \omega_2 = 0$, and hence the accelerated estimation of both f_x and f_p. The lower panels (d) are for the probing of EPR variables $\hat{x}_-$ and $\hat{p}_+$ of two oscillators with opposite, nonvanishing frequencies. All parameters are given in units of the values in Table I.

polynomials in time [38]. The individual terms in these polynomials reflect how the perturbing force affects the measured quantum observable to different order in time. The very long time behavior thus follows from the highest nonvanishing order present in the solution for $\boldsymbol{W}$ and $\boldsymbol{U}$, while lower-order terms with large coefficients may dominate the expressions for shorter times.

The lower panels in Fig. 5(d) show the results for probing EPR variables $\hat{x}_-$ and $\hat{p}_+$ of two oscillators with finite, opposite oscillator frequencies, $\omega_2 = -\omega_1$. These variables are both squeezed, cf., Fig. 4(b), and hence we observe the accelerated estimation of both f_x and f_p, by $\Delta f_i^2 \propto 1/t^3$. For longer times, however, we observe a crossover to a $\Delta f_i^2 \approx \omega^2/(2c_i^2\kappa^2 t)$ asymptotic dependence, which is analyzed further in Appendix E 2.

In practice, the asymptotic behavior shown in Fig. 5 are subject to further change when damping and decoherence are taken into account [38]. This typically replaces the polynomial dependencies on time by exponential convergence to constant values. In the main example of this article we are striving to estimate temporally varying fluctuations, and their variances will typically converge to constant values.

D. Estimation of fluctuating perturbations

When the perturbations are fluctuating in a stochastic manner, early parts of long detection records do not contribute to the estimator at later times and the variances approach final steady-state values. The exact values and rates at which the steady-state variances are approached depend on the measurement scenario as shown in Fig. 6.

In Fig. 6 we assume distinct true initial values for the OU processes, while the estimate assumes vanishing mean values and variances for f_x and f_p, equal to the OU steady-state variances, $\frac{\sigma_x}{2\gamma_x} = \frac{\sigma_p}{2\gamma_p} = 0.05$ in our dimensionless unit.

Figure 6(a) shows results for $\omega_1 = 0$ when we probe only the oscillator quadrature variable affected by f_p. The variance of f_x does not change, while the variance of the probed perturbation f_p converges to a small steady-state value. In Fig. 6(b), we show results when both oscillator quadratures are probed and $\omega_1 = \omega_2 = 0$. Both perturbations are correctly estimated, but with larger variance than for f_p in Fig. 6(a) due to the absence of squeezing. The range of values explored by f_x and f_p are the same, but the faster damping and diffusion of f_x implies that it is more difficult to estimate precisely and hence it shows a larger variance.

Probing both $\hat{x}_-$ and $\hat{p}_+$ for oscillators with $\omega_1 = \omega_2 = 0$ leads to the results shown in Fig. 6(c), where both perturbations have variances that follow a crossover from an initial $1/t^3$ to a small constant variance like for f_p in Fig. 6(a). The same behavior is seen in Fig. 6(d) for the probing of $\hat{x}_-$ and $\hat{p}_+$ for oscillators with opposite, finite frequencies $\omega_2 = -\omega_1$. For the chosen parameters, we reach the constant steady-state values before the crossover between the $1/t^3$and $1/t$ behavior observed in Fig. 5.

The successful demonstration of the efficient real time tracking of both fields using entangled oscillator variables with one positive and one negative evolution frequency constitutes a confirmation of the use of the backaction evading protocol by Tsang and Caves [7,8] and is a main result of this paper.

E. Smoothing

Finally, we apply the theory of past quantum states (35) to retrodict the time-dependent values of the perturbations based on the full measurements records. Such analysis was done for a single perturbation in Ref. [46], and it also applies to the negative mass oscillator setting and simultaneous estimation of two perturbations by two optical probes.

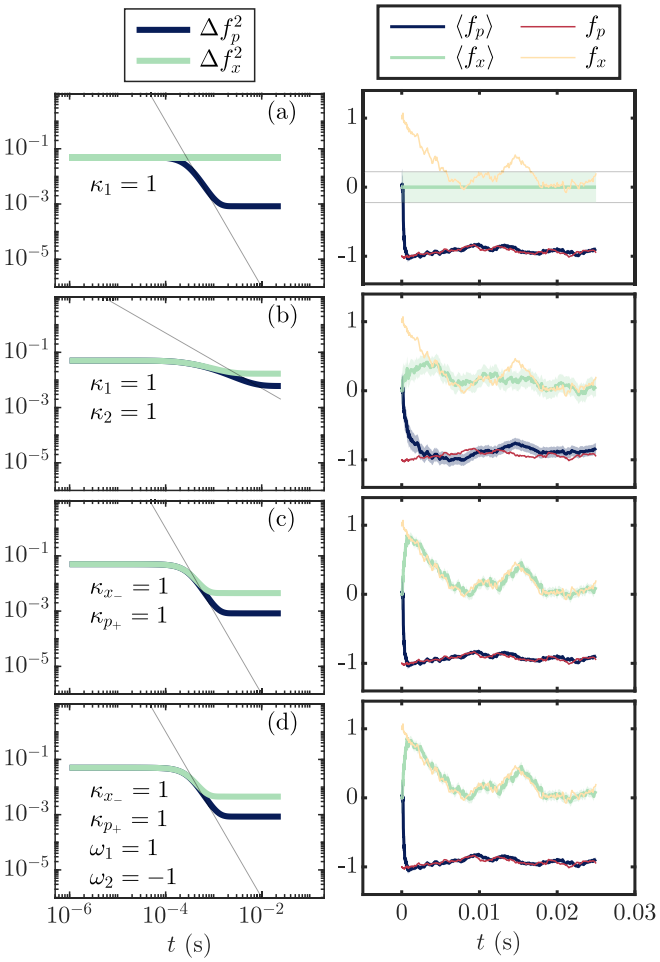

FIG. 6. Estimation of a fluctuating perturbations with $\gamma_{x,p}$ and $\sigma_{x,p}$ given in Table I. The left panels show the variance Δf_i^2 with $1/t$ and $1/t^3$ trend lines. The right panels show the true and estimated perturbation $\langle f_i\rangle \pm \Delta f_i$ (the true values are taken to be large positive and negative to distinguish their estimates clearly in the panels). The upper panels (a) show the results for probing of $\hat{p}_{S_1}$ for a single oscillator with $\omega_1 = 0$ being sensitive to only the value of f_p. Panels (b) show the results for probing of $\hat{x}_{S_1}$ and $\hat{p}_{S_1}$ of a single oscillator with $\omega_1 = 0$, being sensitive to both f_x and f_p, but without the benefit of squeezing of the oscillator. Panels (c) are for the probing and squeezing of EPR variables $\hat{x}_-$ and $\hat{p}_+$ of two oscillators with $\omega_1 = \omega_2 = 0$, and hence the accelerated estimation of both f_x and f_p. The lower panels (d) are for the probing of EPR variables $\hat{x}_-$ and $\hat{p}_+$ of two oscillators with opposite, nonvanishing frequencies. All listed parameters are given in units of the values in Table I. The higher variance of f_x is due to its faster OU damping and fluctuations.

Figure 7 compares the time-dependent f_x smoothed estimate with the true (simulated) time-dependent value, shown as the lighter and darker (most noisy) solid curves. The forward filtering estimate is shown by the dotted data and follows the true time dependence but with a clearly visible delay, while the smoothed estimate (light solid curve) is visibly smoother than the forward filtering estimate, and it does not lag systematically behind the signal. The corresponding estimates match the true perturbation values better which can be quantified by the mean-square error $\overline{[f_i(t) - \langle f_i(t)\rangle]^2}$. With

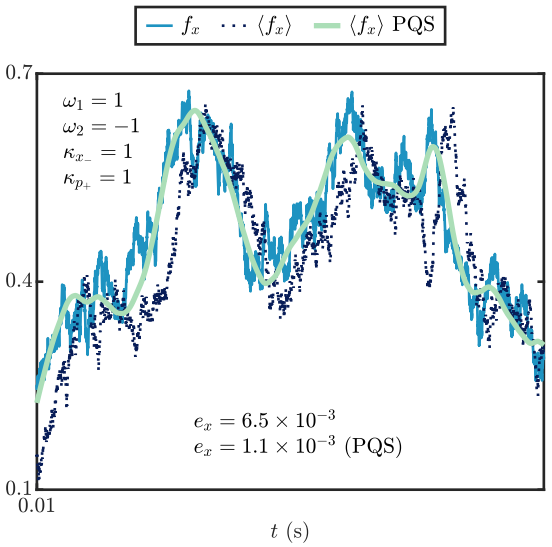

FIG. 7. Perturbation estimation using past quantum states. The mean-square error e_x is recorded from $t_1 = 0.01$ s to $t_2 = T$.

the parameters chosen in Table I, the smoothed estimate leads to a reduction of the mean square error by a factor three to four compared with the forward filter estimate.

V. CONCLUSION

In summary, we have presented a real-time analysis of a backaction evading measurement protocol based on EPR correlations between a probe oscillator and an ancillary negative mass oscillator [8]. Continuous probing of the EPR variables enables their simultaneous squeezing and hence enhanced sensitivity to changes caused by perturbations of the position and momentum quadrature of the probe oscillator. The degree of squeezing of the quantum oscillators, the correlations between the oscillator variables and the perturbations, and the variance of our resulting estimate of the perturbations are all governed by a covariance matrix which obeys a deterministic equation, while their mean values, and hence the estimated value of the perturbation are continuously updated in accordance with the random measurement record. Finally, Bayesian estimates for the perturbations were obtained relying at every instant of time on both earlier and later measurement data. The procedure to describe these smoothed estimates yielded a further reduction in the uncertainty about the actual perturbation.

Our theory builds on the conditional dynamics of a hybrid quantum classical density matrix subject to continuous measurements, and it is significantly simplified by the restriction to Gaussian states throughout the process. This restriction applies well to mechanical and field oscillators, but also to large polarized spin ensembles, and the assumption of interaction Hamiltonians with only quadratic terms applies exactly or to a good approximation for many studies with these systems. We also note that systems with many degrees of freedom such as Bose-Einstein condensates and generic many-body systems may be well described by Bogoliubov theory or second-order cumulant expansion methods and that our Gaussian covariance matrix method can readily deal with a large number of degrees of freedom and hence explore the prospects of

sensing with such complex systems. There is, however, also a rich potential to explore non-Gaussian states for precision measurements [47], and, e.g., the assumption that the classical perturbations obey an Ornstein-Uhlenbeck process may be challenged in many practical sensing applications and hence their representation by Gaussian distributions become invalid. Integration of the hybrid quantum filtering with more pragmatic signal processing models, along the lines of Ref. [36], may then be needed for backaction evading measurements to reach their full potential.

ACKNOWLEDGMENTS

This work was supported by the Danish National Research Foundation through the Center of Excellence for Complex Quantum Systems (Grant Agreement No. DNRF156), the European QuantERA grant C'MON-QSENS! by Innovation Fund Denmark Grant No. 9085-00002, and the European Union's Horizon 2020 Research and Innovation Programme under the Marie Sklodowska-Curie program (754513).

APPENDIX A: OVERVIEW OF THE APPENDICES

These Appendices present supplementary derivations and results of the estimation procedures presented in the main text. Appendix B elaborates on the hybrid quantum-classical description of the system. In Appendix C it is shown that the measurement backaction in the augmented quantum state formalism is fully equivalent to Bayesian inference of the classical perturbations acting on the genuine quantum system. In Appendix D we show that the hybrid Wigner function does not depend on "dummy" quantum conjugate variables to the unknown classical perturbations (the Wigner function is independent of, and has infinite variance in those directions). This allows their exclusion from the formal description of both our forward filter theory and smoothed estimate based on the past quantum state moments. In Appendix E we present some analytical results for the time evolution of quantum state and classical parameter variance.

APPENDIX B: HYBRID QUANTUM AND CLASSICAL GAUSSIAN DISTRIBUTIONS

The most general setup in the main text concerns two oscillators S_1 and S_2 with respective oscillation frequency ω_1 and ω_2 being continuously probed by two light meters L_1 and L_2 where the coupling between S_i and L_j is κ_{ij} for $i, j = 1, 2$. The oscillator variables $\hat{x}_{S_1}$ and $\hat{p}_{S_1}$ are coupled to classical perturbations $f_x(t)$ and $f_p(t)$ with strength c_i for $i = x, p$, while the perturbations evolve in time according to stochastic Ornstein-Uhlenbeck (OU) processes with diffusion σ_i and decay rates γ_i.

The relevant collective Einstein-Podolsky-Rosen (EPR) variables and their variances are related to the individual quantum oscillators S_1 and S_2 by

$$\begin{aligned}\hat{x}_- &= \frac{1}{\sqrt{2}}\big(\hat{x}_{S_1} - \hat{x}_{S_2}\big),\\ \Delta\hat{x}_-^2 &= \frac{1}{2}\big(\Delta\hat{x}_{S_1}^2 + \Delta\hat{x}_{S_2}^2\big) - \Delta\big(\hat{x}_{S_1}, \hat{x}_{S_2}\big),\end{aligned} \tag{B1}$$

$$\begin{aligned}\hat{p}_+ &= \frac{1}{\sqrt{2}}\big(\hat{p}_{S_1} + \hat{p}_{S_2}\big),\\ \Delta\hat{p}_+^2 &= \frac{1}{2}\big(\Delta\hat{p}_{S_1}^2 + \Delta\hat{p}_{S_2}^2\big) + \Delta\big(\hat{p}_{S_1}, \hat{p}_{S_2}\big).\end{aligned} \tag{B2}$$

These EPR variables commute, $[\hat{x}_-, \hat{p}_+] = 0$, and both can be squeezed indefinitely which can be effected by the backaction from the continuous coupling and measurement (successive homodyne detection of temporal segments of the light field). Probing $\hat{p}_+$ ($\hat{x}_-$) is achieved by choosing $\kappa_{11} = \kappa_{21} \equiv \kappa_1$ ($\kappa_{12} = -\kappa_{22} \equiv \kappa_2$). The adverse measurement backaction effects from the antisqueezed conjugate variables $\hat{p}_-, \hat{x}_+$ is evaded by choosing $\omega_1 = -\omega_2$. We assume dimensionless oscillator variables $[\hat{x}_{S_i}, \hat{p}_{S_j}] = i\delta_{i,j}$ and units where effectively $\hbar = 1$.

All the system components are Gaussian elements, i.e., the Wigner function is a multivariate Gaussian, and all the operations preserve the Gaussianity. This affords a compact description in terms of the mean vector $\boldsymbol{a}$ and covariance matrix $\boldsymbol{A}$ and their effective evolution (the sequentially incident light meter subsystems are traced out after each measurement). That is, the elements of $\boldsymbol{a}$ and $\boldsymbol{A}$ are the quantum expectation values and covariances, respectively, of the oscillator variables at time t.

A hybrid classical-quantum formalism is employed to conveniently estimate the classical perturbations. This is achieved by associating the perturbation f_i with eigenstates and eigenvalues of an ancillary quantum operator $\hat{f}_i$, $\hat{f}_i|f_i\rangle = f_i|f_i\rangle$. In our example we deal with two such perturbations, $i = x, p$. The new variables are introduced through an augmented density matrix, $\hat{\tilde{\rho}} = \int |f_x, f_p\rangle\langle f_x, f_p| \otimes \hat{\rho}_{f_x,f_p}\, df_x df_p$, where each $\hat{\rho}_{f_x,f_p}$ is an operator defined on the space of genuine quantum variables and has a time evolution governed by the application of the candidate values of the perturbations and conditioned on the measurement outcomes of the light probes. The joint probability density for f_x and f_p being the true values of the perturbation is given by $P(f_x, f_p) = \mathrm{tr}[\hat{\rho}_{f_x,f_p}]$. Since the total normalization is given by $\hat{\tilde{\rho}}$, each measurement event redistributes the norm between the individual $\hat{\rho}_{f_x,f_p}$, and hence the probabilities, in a Bayesian manner.

To recover a Gaussian description we let the ancillary quantum operators be position operators $\hat{f}_i = \hat{x}_{f_i}$ with conjugate, uncoupled "dummy" variables $\hat{p}_{f_i}$. Then there exists a Wigner function defined on the joint space of all the genuine and ancillary quantum variables. The OU process is described statistically by a Fokker-Planck equation and its diffusion and decay rates can be equivalently imposed on the associated ancillary quantum variables in a Gaussian manner. This results in an augmented mean vector $\tilde{\boldsymbol{a}} = \tilde{\boldsymbol{a}}_\rho$ and covariance matrix $\tilde{\boldsymbol{A}} = \tilde{\boldsymbol{A}}_\rho$, which include the first and second moments of our classical Gaussian estimator of the perturbations.

The values of the perturbations at time t can also be retrodicted based on the entire detection record using the theory of past quantum states. This introduces a backward evolving effect matrix $\hat{\tilde{E}}$ on the same Hilbert space as $\hat{\tilde{\rho}}$ which also has a Gaussian Wigner representation with mean vector $\tilde{\boldsymbol{a}}_E$ and covariance matrix $\tilde{\boldsymbol{A}}_E$. Finally, appropriate combination of the $\hat{\tilde{\rho}}$ and $\hat{\tilde{E}}$ moments yields a vector $\tilde{\boldsymbol{m}}_{\rho,E}$ and a matrix $\tilde{\boldsymbol{A}}_{\rho,E}$. An element of $\tilde{\boldsymbol{m}}_{\rho,E}$ and the corresponding diagonal element of

$\tilde{\boldsymbol{A}}_{\rho,E}$ yield the estimated mean and variance of the outcome of a projective measurement of the corresponding observable. These form our retrodicted Gaussian Bayesian estimator for the elements representing the classical perturbations.

APPENDIX C: AUGMENTED DENSITY MATRIX UPDATES AS BAYESIAN INFERENCE

The classical-quantum hybrid formalism in the main text includes the perturbation f to be estimated as an ancillary quantum operator $\hat{f}$ on equal footing with the genuine quantum operators. This allows a convenient density-matrix ansatz (we consider here a single perturbation and light meter for brevity),

$$\hat{\tilde{\rho}} = \int |f\rangle\langle f| \otimes \hat{\rho}_f \, df = \int |f\rangle\langle f| \otimes \mathrm{tr}[\hat{\rho}_f]\hat{\rho}_f^{(n)} \, df, \quad \text{(C1)}$$

where the normalization of $\hat{\rho}_f$ is explicitly factored, $\hat{\rho}_f = \mathrm{tr}[\hat{\rho}_f]\hat{\rho}_f^{(n)}$. $\mathrm{tr}[\hat{\rho}_f^{(n)}] = 1$ and $\mathrm{tr}[\hat{\rho}_f]$ is the probability density for the perturbation to have the classical value f,

$$\begin{aligned} P(f) &= \mathrm{tr}[|f\rangle\langle f|\hat{\tilde{\rho}}] = \mathrm{tr}\big[|f\rangle\langle f| \otimes \hat{\rho}_f^{(n)}\big]\mathrm{tr}[\hat{\rho}_f] \\ &= \mathrm{tr}[|f\rangle\langle f|]\mathrm{tr}\big[\hat{\rho}_f^{(n)}\big]\mathrm{tr}[\hat{\rho}_f] = \mathrm{tr}[\hat{\rho}_f]. \end{aligned} \quad \text{(C2)}$$

Note here that $\mathrm{tr}[|f\rangle\langle f|] = \int \delta(f - f')^2 \, df$ is technically divergent, in the same manner as the trace of the resulting resolution of the identity operator diverges due to the infinite-dimensional Hilbert space. This issue may be formally dealt with by use of regular approximations to the δ functions and proper truncation of the Hilbert space, and the δ functions and the $|f\rangle\langle f|$ do not pose problems when used in a consistent manner.

The unitary evolution of each $\hat{\rho}_f$ is described by an operator $\hat{U}_f$ where the perturbation takes the definite classical value f. The total unitary evolution operator for $\hat{\tilde{\rho}}$ can then be constructed by

$$\hat{\tilde{U}} = \int |f\rangle\langle f| \otimes \hat{U}_f \, df. \quad \text{(C3)}$$

A unitary evolution alone,

$$\hat{\tilde{U}}\hat{\tilde{\rho}}\hat{\tilde{U}}^\dagger = \int |f\rangle\langle f| \otimes (\hat{U}_f\hat{\rho}^{(\mathrm{n})}\hat{U}_f^\dagger)\,\mathrm{tr}[\hat{\rho}_f]\,df, \quad \text{(C4)}$$

does not change the probability distribution for f,

$$\begin{aligned} P(f) &= \mathrm{tr}[|f\rangle\langle f|(\hat{\tilde{U}}\hat{\tilde{\rho}}\hat{\tilde{U}}^\dagger)] \\ &= \mathrm{tr}[|f\rangle\langle f| \otimes (\hat{U}_f\hat{\rho}\hat{U}_f^\dagger)^{(\mathrm{n})}\,\mathrm{tr}[U_f\hat{\rho}_f U_f^\dagger]] = \mathrm{tr}[\hat{\rho}_f]. \end{aligned} \quad \text{(C5)}$$

Suppose now the unitary evolution is followed by a measurement, $\hat{\Omega}_q = \hat{M}_q\hat{\tilde{U}}$, where $\hat{M}_q$ is the POVM element for the outcome q, then the conditioned state is

$$\hat{\tilde{\rho}}_q = \frac{\hat{M}_q\hat{\tilde{U}}\hat{\tilde{\rho}}\hat{\tilde{U}}^\dagger\hat{M}_q^\dagger}{\mathrm{tr}[\hat{M}_q\hat{\tilde{U}}\hat{\tilde{\rho}}\hat{\tilde{U}}^\dagger\hat{M}_q^\dagger]}. \quad \text{(C6)}$$

The denominator is the probability for detecting the outcome q,

$$\begin{aligned} \mathrm{tr}[\hat{M}_q\tilde{U}\hat{\tilde{\rho}}\tilde{U}^\dagger\hat{M}_q^\dagger] &= \int \mathrm{tr}[\hat{M}_q^\dagger\hat{M}_q(\hat{U}_f\hat{\rho}_f\hat{U}_f^\dagger)^{(\mathrm{n})}]\,\mathrm{tr}[\hat{\rho}_f]\,df \\ &= \int P(q|f)P(f)\,df = P(q). \end{aligned} \quad \text{(C7)}$$

The conditioned state can therefore be written

$$\begin{aligned} \hat{\tilde{\rho}}_q &= \int |f\rangle\langle f| \otimes (\hat{M}_q\hat{U}_f\hat{\rho}_f\hat{U}_f^\dagger\hat{M}_q^\dagger)\frac{1}{P(q)}\,df \\ &= \int |f\rangle\langle f| \otimes \hat{M}_q(\hat{U}_f\hat{\rho}_f\hat{U}_f^\dagger)^{(\mathrm{n})}\hat{M}_q^\dagger\frac{\mathrm{tr}[\hat{\rho}_f]}{P(q)}. \end{aligned} \quad \text{(C8)}$$

Finally, the updated probability distribution for f after detecting q is

$$\begin{aligned} P(f|q) &= \mathrm{tr}[|f\rangle\langle f|\hat{\tilde{\rho}}_q] = \mathrm{tr}[\hat{M}_q^\dagger\hat{M}_q(\hat{U}_f\hat{\rho}_f\hat{U}_f^\dagger)^{(\mathrm{n})}]\frac{\mathrm{tr}[\hat{\rho}_f]}{P(q)} \\ &= \frac{P(q|f)P(f)}{P(q)}, \end{aligned} \quad \text{(C9)}$$

which is exactly Bayes rule. This result generalizes straightforwardly to an arbitrary number of perturbations and probe fields and applies successively as the measurement record accumulates.

APPENDIX D: AUGMENTED DENSITY MATRIX WIGNER FUNCTION

To admit the unknown classical perturbation into the quantum Wigner function description we specify $\hat{f} = \hat{x}_f$ as the position operator of an ancillary system with a conjugate momentum operator $\hat{p}_f$. Then there exists a Wigner function $\mathcal{W}_{\tilde{\rho}}(x, p, x_f, p_f)$ (for simplicity of notation we consider a single perturbation and oscillator).

The ancillary system has a vanishing Hamiltonian and $\hat{p}_f$ does not couple to $\hat{x}_f$ or to the genuine quantum oscillators and will hence play no role in the dynamics. Due to $\hat{\tilde{\rho}}$ being diagonal in the continuous $\hat{x}_f$ eigenbasis, the Wigner function does not depend on the dummy variable,

$$\begin{aligned} \mathcal{W}_{\hat{\tilde{\rho}}}(x, p, x_f, p_f) &= \frac{1}{(\pi\hbar)^2}\int \langle x+q, x_f+q_f|\left(\int dx_f'|x_f'\rangle\langle x_f'| \otimes \hat{\rho}_{f'}\right)|x-q, x_f-q_f\rangle e^{2ipq/\hbar}e^{2ip_fq_f/\hbar}dqdq_f \\ &= \frac{1}{(\pi\hbar)^2}\int \langle x+q|\hat{\rho}_{f'}|x-q\rangle\langle x_f+q_f|x_f''\rangle\langle x_f'|x_f-q_f\rangle e^{2ipq/\hbar}e^{2ip_fq_f/\hbar}dqdq_fdx_f' \\ &= \frac{1}{(\pi\hbar)^2}\int \langle x+q|\hat{\rho}_f|x-q\rangle e^{2ipq/\hbar}dq \times \delta((x_f-x_f')+q_f)\delta((x_f-x_f')-q_f)e^{2ip_fq_f/\hbar}dq_fdx_f'. \end{aligned} \quad \text{(D1)}$$

The two δ functions imply that the integral only acquires contributions for $x_f = x_f'$ and $q_f = 0$ and hence it is independent of p_f and sifts out the dependence of ρ_f on f. For Gaussian states this implies infinite variance in the p_f direction, which

however, plays no role in the dynamics. Being independent of p_f also implies that we do not need to retain the argument in the Wigner function and in the mean values and covariances. Generalizing to multiple perturbations and returning to the $\boldsymbol{f}$ notation, we hence specify only the effective $\mathcal{W}_{\tilde{\rho}}(\boldsymbol{x}, \boldsymbol{p}, \boldsymbol{f})$ and associated joint Gaussian moments $\tilde{\boldsymbol{a}}_\rho$ and $\tilde{\boldsymbol{A}}_\rho$ for the ancillary and genuine quantum oscillators.

In the retrodictive past quantum state theory we had recourse to the Wigner function for the effect matrix, $\mathcal{W}_{\tilde{E}}(x, p, f, p_f)$, parametrized by a covariance matrix $\tilde{\boldsymbol{A}}_E$ and mean vector $\tilde{\boldsymbol{a}}_E$. To calculate the probability distribution $P_{\rm pqs}(f)$ conditioned on the entire detection record, it was necessary to determine Wigner functions for operators $|f'\rangle\langle f'|\hat{\tilde{X}}$ with $X = \rho, E$. Since $\hat{\tilde{\rho}}$ and $\hat{\tilde{E}}$ are both diagonal in the $|f\rangle$ basis, the same holds for $|f'\rangle\langle f'|\hat{\tilde{X}}$, and their Wigner functions are both independent of p_f and they evaluate readily to

$$\mathcal{W}_{|f'\rangle\langle f'|\tilde{\rho}}(x, p, f) = \delta(f - f')\mathcal{W}_{\tilde{\rho}}(x, p, f'), \tag{D2}$$

with a similar result for $\hat{\tilde{E}}$ and straightforward generalization to more oscillators and perturbations.

APPENDIX E: NUMERICAL AND ANALYTICAL RESULTS

The evolution of the Gaussian covariance matrix and mean values due to the measurement of the quadrature variables of the probe field follows from the reduction of their joint quantum state by the measurement process. The Gaussian state formalism thus yields discrete analytical update formulas for the covariance matrix $\boldsymbol{A}$ and mean vector $\boldsymbol{a}$ (the "$\sim$" notation is omitted for brevity). The covariance matrix evolves independently of the actual measurement outcomes and in the limit of frequent probing, it solves a so-called Riccati matrix differential equation,

$$\begin{aligned}\dot{\boldsymbol{A}} &= \lim_{\delta t \to 0^+} \frac{\boldsymbol{A}(t + \delta t) - \boldsymbol{A}(t)}{\delta t} \\ &\equiv \boldsymbol{G} - \boldsymbol{D}\boldsymbol{A} - \boldsymbol{A}\boldsymbol{E} - \boldsymbol{A}\boldsymbol{F}\boldsymbol{A},\end{aligned} \tag{E1}$$

where, for our system, the matrices $\boldsymbol{G}, \boldsymbol{D}, \boldsymbol{E}, \boldsymbol{F}$ follow from the infinitesimal linear transformation of the Gaussian variables given in the main text,

$$\boldsymbol{G} = \begin{pmatrix} \kappa_{11}^2 & 0 & \kappa_{11}\kappa_{21} & 0 & 0 & 0 \\ 0 & \kappa_{12}^2 & 0 & \kappa_{12}\kappa_{22} & 0 & 0 \\ \kappa_{11}\kappa_{21} & 0 & \kappa_{21}^2 & 0 & 0 & 0 \\ 0 & \kappa_{12}\kappa_{22} & 0 & \kappa_{22}^2 & 0 & 0 \\ 0 & 0 & 0 & 0 & 2\sigma_x & 0 \\ 0 & 0 & 0 & 0 & 0 & 2\sigma_p \end{pmatrix},$$

$$\boldsymbol{D} = \begin{pmatrix} 0 & -\omega_1 & 0 & 0 & -c_x & 0 \\ \omega_1 & 0 & 0 & 0 & 0 & -c_p \\ 0 & 0 & 0 & -\omega_2 & 0 & 0 \\ 0 & 0 & \omega_2 & 0 & 0 & 0 \\ 0 & 0 & 0 & 0 & \gamma_x & 0 \\ 0 & 0 & 0 & 0 & 0 & \gamma_p \end{pmatrix}, \tag{E2}$$

$$\boldsymbol{E} = \begin{pmatrix} 0 & \omega_1 & 0 & 0 & 0 & 0 \\ -\omega_1 & 0 & 0 & 0 & 0 & 0 \\ 0 & 0 & 0 & \omega_2 & 0 & 0 \\ 0 & 0 & -\omega_2 & 0 & 0 & 0 \\ -c_x & 0 & 0 & 0 & \gamma_x & 0 \\ 0 & -c_p & 0 & 0 & 0 & \gamma_p \end{pmatrix},$$

$$\boldsymbol{F} = \begin{pmatrix} \kappa_{12}^2 & 0 & \kappa_{12}\kappa_{22} & 0 & 0 & 0 \\ 0 & \kappa_{11}^2 & 0 & \kappa_{11}\kappa_{21} & 0 & 0 \\ \kappa_{12}\kappa_{22} & 0 & \kappa_{22}^2 & 0 & 0 & 0 \\ 0 & \kappa_{11}\kappa_{21} & 0 & \kappa_{21}^2 & 0 & 0 \\ 0 & 0 & 0 & 0 & 0 & 0 \\ 0 & 0 & 0 & 0 & 0 & 0 \end{pmatrix}. \tag{E3}$$

This is a nonlinear matrix equation for $\boldsymbol{A}$, but by writing $\boldsymbol{A} = \boldsymbol{W}\boldsymbol{U}^{-1}$ it can be decomposed into two linear matrix equations $\dot{\boldsymbol{W}} = -\boldsymbol{D}\boldsymbol{W} + \boldsymbol{G}\boldsymbol{U}$ and $\dot{\boldsymbol{U}} = \boldsymbol{F}\boldsymbol{W} + \boldsymbol{E}\boldsymbol{U}$. It is generally quite challenging to find closed-form solutions for $\boldsymbol{A}$, but we shall consider a few interesting limiting cases that illuminate our numerical findings.

1. Squeezing by probing

When there are no perturbations present, the last two rows and columns can be removed from the Riccati matrices. We assume that the oscillator variables are initially uncorrelated with ground-state variances, $[\boldsymbol{A}(0)]_{i,j} = \delta_{i,j}$, and we assume $\omega_1 = \omega = -\omega_2$, $\kappa_{11} = \kappa_{21} \equiv \kappa_1$, and $\kappa_{12} = -\kappa_{22} \equiv \kappa_2$.

Defining $K_\pm^2 = \kappa_2^2 \pm \kappa_1^2$, the time-dependent EPR variances can be found and read

$$\Delta\hat{x}_-^2(t) = \frac{\Delta\hat{x}_-^2 + (\Delta\hat{p}_+^2 - \Delta\hat{x}_-^2)\sin^2\omega t + 2\Delta\hat{x}_-^2\Delta\hat{p}_+^2\left[K_+^2 t - \frac{\sin 2\omega t}{2\omega}K_-^2\right]}{[1 + 2\Delta\hat{x}_-^2 K_+^2 t][1 + 2\Delta\hat{p}_+^2 K_+^2 t] + \frac{\sin\omega t}{\omega}K_-\left[\cos\omega t(\Delta\hat{x}_-^2 - \Delta\hat{p}_+^2) - \frac{\sin\omega t}{\omega}K_-\Delta\hat{x}_-^2\Delta\hat{p}_+^2\right]}, \tag{E4}$$

$$\Delta\hat{p}_+^2(t) = \frac{\Delta\hat{p}_+^2 + (\Delta\hat{x}_-^2 - \Delta\hat{p}_+^2)\sin^2\omega t + 2\Delta\hat{x}_-^2\Delta\hat{p}_+^2\left[K_+^2 t + \frac{\sin 2\omega t}{2\omega}K_-^2\right]}{[1 + 2\Delta\hat{x}_-^2 K_+^2 t][1 + 2\Delta\hat{p}_+^2 K_+^2 t] + \frac{\sin\omega t}{\omega}K_-\left[\cos\omega t(\Delta\hat{x}_-^2 - \Delta\hat{p}_+^2) - \frac{\sin\omega t}{\omega}K_-\Delta\hat{x}_-^2\Delta\hat{p}_+^2\right]}, \tag{E5}$$

where $\Delta\hat{x}_-^2$ and $\Delta\hat{p}_+^2$ on the right-hand side are evaluated at $t = 0$, and may be set to $1/2$ by assuming initial oscillator ground states. For nonvanishing ω, the asymptotic behavior is the same for the two variables, $\Delta\hat{x}_-^2(t),\ \Delta\hat{p}_+^2(t) \propto (2K_+^2 t)^{-1}$. The equations apply for all values of ω, while $\lim_{\omega\to 0}\sin(\omega t)/\omega{=}t$ must be applied and yields different asymptotic variances if different probing strengths are applied to the case of $\omega = 0$.

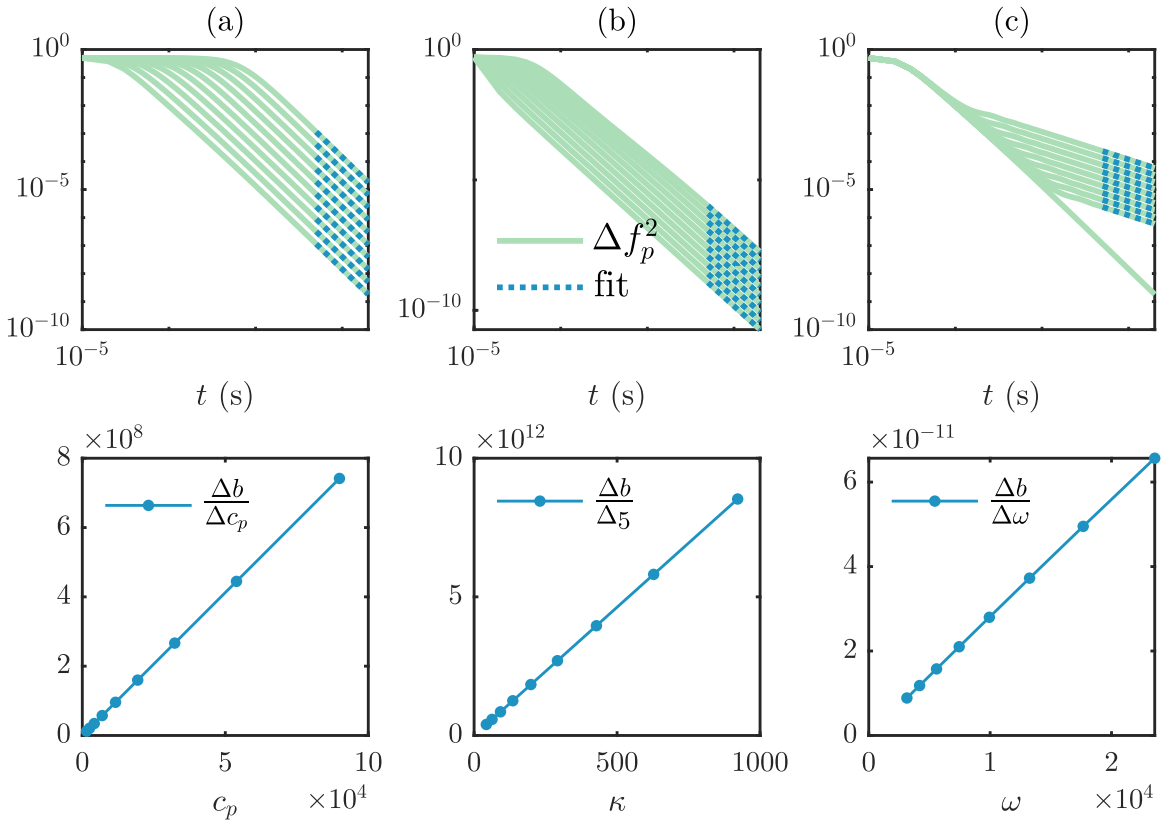

FIG. 8. This figure shows the asymptotic behavior of $\Delta f_p^2(t)$ in the upper parts of the panels. Each point in the lower panels is extracted from one of the curve fits for late times in the upper panels. The lower part of panel (a) shows, for $\omega = 0$, the variation with the perturbation parameter c_p of the fit of the asymptotic (rightmost) results to $1/(bt^3)$. The lower panel (b) shows the variation of the same fit as function of the probing strength parameter κ. Panel (c) shows the variation of the fit of the upper panel results with b/t as function of ω.

2. Estimation of a constant perturbation

The case of separately probing two constant perturbations by the EPR variables is equivalent to the probing of a single constant perturbation and we get a similar result as in Ref. [35] if we assume that the quantum oscillator variables have variances of $1/2$, $[\boldsymbol{A}(0)]_{i,j} = \delta_{i,j}$, and that $\omega_1 = \omega_2 = 0$, while $\kappa_{11} = \kappa_{21} \equiv \kappa_1$ and $\kappa_{12} = -\kappa_{22} \equiv \kappa_2$,

$$\Delta f_p^2(t) = \frac{\left(1 + 2\kappa_1^2 t\right)\Delta f_p^2}{1 + 2\kappa_1^2 t + \frac{2}{3}\kappa_1^2 c_p^2 \Delta f_p^2 t^3 + \frac{1}{3}\kappa_1^4 c_p^2 \Delta f_p^2 t^4} \overset{t\to\infty}{\approx} \frac{6}{c^2 k_1^2}\frac{1}{t^3}, \tag{E6}$$

where Δf_p^2 on the right-hand side is evaluated at $t = 0$, and an equivalent expression applies for $\Delta f_x^2(t)$.

We are not able to solve the case of $\omega_1 = -\omega_2 \neq 0$ analytically. However, for large enough t a crossover from $1/t^3$ to $1/t$ is observed in our numerical calculations in the main text. This suggests the presence of an additional ω-dependent t^3 term in the numerator of Eq. (E6), and, by fitting the asymptotic behavior for different parameter values, Fig. 8 indicates that this ω dependence is quadratic, and for $\omega \neq 0$, $\Delta f_p^2(t) \overset{t\to\infty}{\approx} \omega^2/(2c_p^2\kappa_1^2 t)$.

[1] V. B. Braginsky, Y. I. Vorontsov, and K. S. Thorne, Quantum nondemolition measurements, Science **209**, 547 (1980).

[2] C. M. Caves, K. S. Thorne, R. W. P. Drever, V. D. Sandberg, and M. Zimmermann, On the measurement of a weak classical force coupled to a quantum-mechanical oscillator. I. Issues of principle, Rev. Mod. Phys. **52**, 341 (1980).

[3] V. B. Braginsky and F. Y. Khalili, Quantum nondemolition measurements: The route from toys to tools, Rev. Mod. Phys. **68**, 1 (1996).

[4] M. F. Bocko and R. Onofrio, On the measurement of a weak classical force coupled to a harmonic oscillator: Experimental progress, Rev. Mod. Phys. **68**, 755 (1996).

[5] M. Tse, H. Yu, N. Kijbunchoo, A. Fernandez-Galiana, P. Dupej, L. Barsotti, C. D. Blair, D. D. Brown, S. E. Dwyer, A. Effler, M. Evans, P. Fritschel, V. V. Frolov, A. C. Green, G. L. Mansell, F. Matichard, N. Mavalvala, D. E. McClelland, L. McCuller, T. McRae *et al.*, Quantum-Enhanced Advanced LIGO Detectors in the Era of Gravitational-Wave Astronomy, Phys. Rev. Lett. **123**, 231107 (2019).

[6] G. Vasilakis, H. Shen, K. Jensen, M. Balabas, D. Salart, B. Chen, and E. S. Polzik, Generation of a squeezed state of an oscillator by stroboscopic back-action-evading measurement, Nat. Phys. **11**, 389 (2015).

[7] M. Tsang and C. M. Caves, Coherent Quantum-Noise Cancellation for Optomechanical Sensors, Phys. Rev. Lett. **105**, 123601 (2010).

[8] M. Tsang and C. M. Caves, Evading Quantum Mechanics: Engineering a Classical Subsystem within a Quantum Environment, Phys. Rev. X **2**, 031016 (2012).

[9] M. J. Woolley and A. A. Clerk, Two-mode back-action-evading measurements in cavity optomechanics, Phys. Rev. A **87**, 063846 (2013).

[10] K. Zhang, P. Meystre, and W. Zhang, Back-action-free quantum optomechanics with negative-mass Bose-Einstein condensates, Phys. Rev. A **88**, 043632 (2013).

[11] A. Motazedifard, F. Bemani, M. Naderi, R. Roknizadeh, and D. Vitali, Force sensing based on coherent quantum noise cancellation in a hybrid optomechanical cavity with squeezed-vacuum injection, New J. Phys. **18**, 073040 (2016).

[12] H. Allahverdi, A. Motazedifard, A. Dalafi, D. Vitali, and M. H. Naderi, Homodyne coherent quantum noise cancellation in a hybrid optomechanical force sensor, Phys. Rev. A **106**, 023107 (2022).

[13] A. Einstein, B. Podolsky, and N. Rosen, Can quantum-mechanical description of physical reality be considered complete? Phys. Rev. **47**, 777 (1935).

[14] K. Hammerer, M. Aspelmeyer, E. S. Polzik, and P. Zoller, Establishing Einstein-Podolsky-Rosen Channels between Nanomechanics and Atomic Ensembles, Phys. Rev. Lett. **102**, 020501 (2009).

[15] W. Wasilewski, K. Jensen, H. Krauter, J. J. Renema, M. V. Balabas, and E. S. Polzik, Quantum Noise Limited and Entanglement-Assisted Magnetometry, Phys. Rev. Lett. **104**, 133601 (2010).

[16] E. S. Polzik and K. Hammerer, Trajectories without quantum uncertainties, Ann. Phys. (Berlin, Ger.) **527**, A15 (2015).

[17] C. B. Møller, R. A. Thomas, G. Vasilakis, E. Zeuthen, Y. Tsaturyan, M. Balabas, K. Jensen, A. Schliesser, K. Hammerer, and E. S. Polzik, Quantum back-action-evading measurement of motion in a negative mass reference frame, Nature (London) **547**, 191 (2017).

[18] G. Adesso, S. Ragy, and A. R. Lee, Continuous variable quantum information: Gaussian states and beyond, Open Systems & Information Dynamics **21**, 1440001 (2014).

[19] M. Tsang, Time-Symmetric Quantum Theory of Smoothing, Phys. Rev. Lett. **102**, 250403 (2009).

[20] M. Tsang, Optimal waveform estimation for classical and quantum systems via time-symmetric smoothing, Phys. Rev. A **80**, 033840 (2009).

[21] M. Tsang, Optimal waveform estimation for classical and quantum systems via time-symmetric smoothing. II. Applications to atomic magnetometry and Hardy's paradox, Phys. Rev. A **81**, 013824 (2010).

[22] P. S. Maybeck, *Stochastic Models, Estimation, and Control* (Academic Press, New York, San Francisco, London, 1979).

[23] D. Q. Mayne, A solution of the smoothing problem for linear dynamic systems, Automatica **4**, 73 (1966).

[24] D. C. Fraser and J. L. Potter, The optimum linear smoother as a combination of two optimum linear filters, IEEE Trans. Autom. Control **14**, 387 (1969).

[25] F. Verstraete, A. C. Doherty, and H. Mabuchi, Sensitivity optimization in quantum parameter estimation, Phys. Rev. A **64**, 032111 (2001).

[26] C. M. Caves and G. J. Milburn, Quantum-mechanical model for continuous position measurements, Phys. Rev. A **36**, 5543 (1987).

[27] V. P. Belavkin, Continuous non-demolition observation quantum filtering and optimal estimation, in *Quantum Aspects of Optical Communications*, edited by C. Bendjaballah, O. Hirota, and S. Reynaud (Springer, Berlin, Heidelberg, 1991), pp. 151–163.

[28] H. Mabuchi, Dynamical identification of open quantum systems, Quantum Semiclassical Opt. **8**, 1103 (1996).

[29] J. Gambetta and H. M. Wiseman, State and dynamical parameter estimation for open quantum systems, Phys. Rev. A **64**, 042105 (2001).

[30] M. L. Eaton, *Multivariate Statistics: A Vector Space Approach* (John Wiley & Sons, Inc., New York, 1983).

[31] J. Eisert, S. Scheel, and M. B. Plenio, Distilling Gaussian States with Gaussian Operations is Impossible, Phys. Rev. Lett. **89**, 137903 (2002).

[32] L. Madsen and K. Mølmer, Gaussian description of continuous measurements on continuous variable quantum systems, in *Quantum Information with Continuous Variables of Atoms and Light*, edited by N. Cerf, G. Leuchs, and E. Polzik (Imperial College Press, 2007).

[33] C. N. Madsen, L. Valdetaro, and K. Mølmer, Quantum estimation of a time-dependent perturbation, Phys. Rev. A **104**, 052621 (2021).

[34] JM Geremia, J. K. Stockton, A. C. Doherty, and H. Mabuchi, Quantum Kalman Filtering and the Heisenberg Limit in Atomic Magnetometry, Phys. Rev. Lett. **91**, 250801 (2003).

[35] K. Mølmer and L. B. Madsen, Estimation of a classical parameter with Gaussian probes: Magnetometry with collective atomic spins, Phys. Rev. A **70**, 052102 (2004).

[36] R. Jiménez-Martínez, J. Kołodyński, C. Troullinou, V. G. Lucivero, J. Kong, and M. W. Mitchell, Signal Tracking Beyond the Time Resolution of an Atomic Sensor by Kalman Filtering, Phys. Rev. Lett. **120**, 040503 (2018).

[37] J. Amorós-Binefa and J. Kołodyński, Noisy atomic magnetometry in real time, New J. Phys. **23**, 123030 (2021).

[38] L. B. Madsen and K. Mølmer, Spin squeezing and precision probing with light and samples of atoms in the Gaussian description, Phys. Rev. A **70**, 052324 (2004).

[39] L. Rabiner, A tutorial on hidden Markov models and selected applications in speech recognition, Proc. IEEE **77**, 257 (1989).

[40] S. Gammelmark, B. Julsgaard, and K. Mølmer, Past Quantum States of a Monitored System, Phys. Rev. Lett. **111**, 160401 (2013).

[41] S. Watanabe, Symmetry of physical laws. Part III. Prediction and retrodiction, Rev. Mod. Phys. **27**, 179 (1955).

[42] Y. Aharonov, P. G. Bergmann, and J. L. Lebowitz, Time symmetry in the quantum process of measurement, Phys. Rev. **134**, B1410 (1964).

[43] B. Reznik and Y. Aharonov, Time-symmetric formulation of quantum mechanics, Phys. Rev. A **52**, 2538 (1995).

[44] M. A. Nielsen and I. L. Chuang, *Quantum Computation and Quantum Information: 10th Anniversary Edition* (Cambridge University Press, Cambridge, 2010).

[45] R. A. Thomas, M. Parniak, C. Østfeldt, C. B. Møller, C. Bærentsen, Y. Tsaturyan, A. Schliesser, J. Appel, E. Zeuthen, and E. S. Polzik, Entanglement between distant macroscopic mechanical and spin systems, Nat. Phys. **17**, 228 (2021).

[46] C. Zhang and K. Mølmer, Estimating a fluctuating magnetic field with a continuously monitored atomic ensemble, Phys. Rev. A **102**, 063716 (2020).

[47] A. Evrard, V. Makhalov, T. Chalopin, L. A. Sidorenkov, J. Dalibard, R. Lopes, and S. Nascimbene, Enhanced Magnetic Sensitivity with Non-Gaussian Quantum Fluctuations, Phys. Rev. Lett. **122**, 173601 (2019).